MiR-302a reprogrammed fibroblast-derived induced anti-aging neural stem cells improve cognition and prolong lifespan in Alzheimer's disease model

Yuanyuan Li
Binzhou Medical University
Jing Sun
Binzhou Medical University
Yuanyuan Zheng
Binzhou Medical University
Tingting Xu
Binzhou Medical University
Yanan Zhang
Binzhou Medical University
Yuesi Wang (wangyuesi@bzmc.edu.cn)
Binzhou Medical University

Research Article

Keywords: Induced neural stem cells, Anti-aging, Alzheimer's, Cognitive, Prolong lifespan

Posted Date: June 5th, 2023

DOI: https://doi.org/10.21203/rs.3.rs-3005271/v1

Additional Declarations: No competing interests reported.

Abstract

Background: Neural stem cells (NSC) are essential for maintaining tissue homeostasis and promoting longevity in living organisms. As a promising approach to treating neurodegenerative diseases, NSC transplantation has been hampered by crucial issues such as cellular senescence, immune rejection, and low cell viability.

Methods: MiR-302a was used to reprogram human and mouse fibroblast cells into induced neural stem cells (iNSCs). In vitro, differentiation experiments were performed to demonstrate that iNSCs have the ability to differentiate into neurons, astrocytes, and oligodendrocytes. INSCs were transplanted into nude mice to evaluate cell survival, differentiation, and tumor formation in vivo. Multi-electrode arrays were used to determine that the differentiated neurons from iNSCs have mature electrophysiological functions. INSCs were treated with oxidative damage to test their antioxidant and anti-aging abilities. The supernatant of iNSCs was used to treat aged cells to determine their antioxidant and anti-aging effects. INSCs were transplanted into SAMP8 rapid aging Alzheimer's disease (AD) mouse model for behavioral tests to evaluate the improvement and therapeutic effects of iNSCs treatment on cognitive function and memory. Tests were also performed to assess lifespan extension, improved glycemic control, promoted motor ability recovery, improved reproductive ability, and improved hearing.

Results: We report that a single miR-302 factor alone can effectively reprogram human and mouse fibroblasts directly into iNSCs within 2-3 days, confirmed by cell phenotype, molecular characterization, and functional analysis. The anti-aging factors Nrf2, Sirt6, and Foxo3 are highly expressed in induced neural stem cells reprogrammed by miR-302a (miR-302a-hiNSCs). Compared to other iNSCs, miR-302a-hiNSCs showed delayed aging and increased resilience to oxidative stress. MiR-302a-hiNSCs were implanted into SAMP8 mice to improve cognition, extend longevity by 40.625%, increase fatigue resistance, and enhance blood sugar control, hair regrowth, and reproduction.

Conclusion: Our study highlights the potential of iNSCs generated based on miR-302a as a promising therapeutic approach for treating various age-related diseases and conditions. We found the iNSCs treatment to improve lifespan, cognitive abilities in late-stage AD, fatigue resistance, hair regeneration, blood glucose, and fat metabolism, renal function, reproductive function, and hearing loss.

Background

The aging process is a multifaceted and complex phenomenon characterized by a chronic dysregulation of cellular behavior leading to a decline in tissue and organ function, resulting in various degenerative diseases, including Alzheimer's disease (AD), frailty, and tumors [1, 2]. Despite the decline in adult neurogenesis, which is the process of generating neurons in the adult brain, it continues to persist throughout life and is a critical component in the occurrence of diseases such as Alzheimer's syndrome. As a result, it serves as a potential target for prolonging cognitive health and reducing the risk of neurodegenerative diseases. With the increasing life expectancy, the prevalence of these health

challenges is becoming more apparent, emphasizing the need for effective interventions [3–6]. The age-related loss of neural stem cell (NSC) numbers and/or activity is believed to play a critical role in the decline of brain function [5, 7–10]. Hippocampal neural stem cells (NSCs) are particularly susceptible to cellular senescence [11], and disruption of the persistence of these cells in the hypothalamus has been shown to accelerate aging in mice [12]. Therefore, interventions aimed at reversing NSC aging may increase the period of cognitive health in humans.

Some researchers have suggested that a decline in the function of the central nervous system (CNS) is one of the principal markers of aging in mammals [13]. Although there has been considerable advancement in the field and continuous study, a cure for this chronic illness still has not been discovered. As a result, such declines in cell number or function may be susceptible to interventions aimed at slowing or preventing aging while also delaying or preventing other diseases and thus extending a healthy lifespan. An attractive theory is to say that the decline in brain function with age is the result of loss of stem cell numbers and/or activity, then an intervention that supplements stem cell numbers or reverses stem cell aging may extend the human lifespan and health span [14].

Because stem cell transplantation has the capacity to exert numerous restorative effects, including cell replacement and paracrine effects, it appears to be a promising treatment approach for neurodegenerative illnesses such as AD and aging [15, 16]. However, most preclinical studies and clinical trials use allogeneic mesenchymal stem cells (MSCs), NSCs, or induced pluripotent stem cells (iPSCs). Due to limited expansion of mesenchymal stem cells and other cells in vitro, increased aging cells during later passages, heterogeneous cell sources, and poor preservation and survival rates of transplanted MSCs in vivo that rapidly deteriorate under stress responses in vivo and can hardly resist adverse environments in the brain, this treatment is not the best method. In addition, iPS cells or gene editing still carry risks of carcinogenesis, which also hinders the widespread application of these stem cell transplantation technologies. Autologous patient-derived NSC therapies may have significant advantages for clinical use [17]. The capacity of autologous NSC transplantation to escape immune rejection not only reduces the difficulties of immunosuppressive medication, but also increases the visibility of the cells and the therapy's endurance. Research advances in direct cellular reprogramming offer the possibility of developing patient-specific cellular therapies. Induced neural stem cells (iNSCs) have been derived by reprogramming somatic cells with multiple transcription factors and other methods to avoid the pluripotent phase of induced pluripotent stem cells and the risks associated with low differentiation efficiency and carcinogenicity [18–27]. Jing Nai-Ho et al used peripheral blood mononuclear cells (PBMC) reprogrammed as induced NSCs to rescue AD cognitive deficits by strengthening synaptic networks. However, the impact of iNSCs treatment generated by direct reprogramming on the health span of older organisms has not been explored [14]. Cell replacement therapy has excellent therapeutic prospects for restoring tissue homeostasis. However, before cell therapy can be effectively and safely implemented in clinical settings, functional decline and tumorigenesis associated with aging after transplantation must be overcome. This goal can be achieved by developing enhancement strategies that endow stem cells with more vital regenerative abilities while reducing tumorigenicity.

Here we provide experimental and conceptual strategies on how to genetically engineer superior and safer stem cells by direct reprogramming techniques. As a first step towards the development of personalized human-induced NSCs (hiNSCs) therapies, we show that a single miR-302a reprogramming strategy can efficiently and quickly reprogram human dermal fibroblasts into iNSCs in as little as 2–3 days, as evidenced by surface marker, molecular, and functional analysis of the cells. We then show that miR-302a-hiNSCs have better anti-aging and antioxidant functions than other NSC sources. MiR-302a-hiNSCs overexpressing Sirt6, Nrf2, and Foxo3 genes can delay aging and resist external oxidative stress. They are super stem cells that resist aging and stressful environments. In this study, researchers transplanted miR-302a-hiNSCs into 13.5-month-old SAMP8 mice only once. Four months after transplantation, many GFP-positive cells were still found in the hippocampal DG area, significantly reducing the number of transplantations and pain. They can differentiate into neurons, extend lifespan by 40.625%, and no tumors were found. We show that miR-302a-hiNSC hippocampal transplantation significantly improves cognitive function in rapidly aging older SAMP8 mice. Elderly mice receiving miR-302a-hiNSC showed lower levels of frailty and significant improvements in lifespan extension, running wheel testing, glucose regulation, fur regeneration, and renal function. In addition, SAMP8 mice transplanted with iNSCs showed some improvement in hearing compared to the control SAMP8 group. In this report, we sought to identify strategies based on miR-302a reprogramming to obtain iNSCs with high antioxidant and anti-aging capacity to provide a faster and more efficient method of iNSCs acquisition for application in research and clinical therapy.

Materials and methods

Human Samples

Fresh human foreskin samples from two healthy male donors (at the age of 26 and 29) were collected from Yuhuangding Hospital at Yantai, and fresh human eyelid sample from a healthy female donor (at the age of 41) was collected from Chang'an Hospital at Xi'an. All the procedures were performed according to an IRB-approved protocol of either Binzhou Medical University or Northwestern Polytechnical University. The primary foreskin or eyelid cells were cut into pieces with ophthalmic scissors, enzymatically disassociated with (0.25% trypsin, 30 ~ 60 min), and cultured in fibroblasts culture medium, DMEM-High Glucose with 1% penicillin/streptomycin, 2 nM L-glutamine, and 10% FBS.

Viral plasmid construction

The pGLV3-miR-302a plasmid was constructed using the lentiviral vector pGLV3/H1/GFP + Puro (pGLV3; Shanghai GenePharma Co., Ltd., Shanghai, China). The ADV3-U6-has-miR-302a-CMV-GFP overexpression adenoviral vectors plasmid also was constructed by Shanghai GenePharma Co., Ltd. The following sequence was used: miR-302a, 5´-TAAGTGCTTCCATGTTTTGGTGA-3´.

Human and mouse iNSCs generation

Human fibroblasts isolated from the specimens were all expanded in the medium [DMEM/HIGH GLUCOSE + 10% FBS + 1% L-Glutamine + 1% penicillin/streptomycin]. Human fibroblasts, derived from the foreskin or eyelid (at passages 3–10), were grown on glass coverslips coated with gelatin in a 24-well plate at a density of 1 x 10^4 cells per well in fibroblast culture medium. The following day, the medium was replaced with a fresh medium containing the miR-302a virus, polybrene (6 µl), and VPA (10 µg). Twenty-four hours post-transfection, Vitamin C (20 ug) was added within NSCs induction media 500 ul (DMEM/F12 + 2% B27 + 20 ng bFGF + 10 ng/mL EGF + 1% DOX + 1% L-glutamine + 1% penicillin/streptomycin). After 72 h, Puromycin (10 uM) was added to remove untransfected cells, and then the media were changed into NSCs culture media (DMEM/F12 + 2% B27 + 20 ng/mL bFGF + 20 ng/mL EGF + 1% L-glutamine + 1% penicillin/streptomycin). The medium was changed every two days. From 24 h after transfection, some fibroblast morphology changed, and a few small colonies formed and expanded.

Mouse L929 cells were purchased from the ATCC and expanded in the MEF medium [DMEM/HIGH GLUCOSE (Hyclone) + 10% FBS (Gibco) + 1% L-Glutamine + 1% penicillin-streptomycin]. The procedure for the induction of mouse iNSCs (miNSCs) from L929 cells with miR-302a is essentially the same as for human iNSCs (hiNSCs). Mouse L929 cells were purchased from the ATCC and expanded in the MEF medium [DMEM/HIGH GLUCOSE (Hyclone) + 10% FBS (Gibco) + 1% L-Glutamine + 1% penicillin-streptomycin]. The procedure for the induction of mouse iNSCs (miNSCs) from L929 cells with miR-302a is essentially the same as for human iNSCs (hiNSCs).

Real-time quantitative polymerase chain reaction (RT-qPCR)

Total RNA was isolated from iNSCs with the TaKaRa kit (Catalog# RR820A). RT-qPCR was performed with The Light cycle 96 Real-Time PCR System (Roche). The PCR-program: 95°C 30s, 95°C 5s, 60°C 30s. Steps 2–3 were repeated 40 ~ 45 times.

Differentiation of hiNSCs and miNSCs

(1) Astrocytes differentiation: First, a 12-well plate was coated with 40 ug/mL poly-lysine for 1 hour at 37ºC and washed with PBS 3 times. Then hiNSCs were plated onto those polylysine-coated wells, and astrocytes culture medium (DMEM/F12 medium supplemented with 10% FBS, 1×NEAA, and two mM L-glutamine) was applied after hiNSCs attached to the bottom. (2) Oligodendrocytes differentiation: hiNSCs were enzymatically disrupted into single cells with trypsin in a 37°C incubator for 2 min and then resuspended and seeded onto a polylysine-coated glass coverslip and cultured in DMEM/F12 with 1×N2, ten ng/ml PDGF, and three uM forskolin, half of the medium was changed every two days. Four days later, forskolin was substituted with 200 mM VC and cultured for seven days. (3) Neuron differentiation: For the generation of terminally differentiated neurons from hiNSCs, the cells were seeded at a density of 1×10^4 cells per 12 mm glass coverslip coated with poly-ornithine/laminin in the neural induction medium (Neurobasal medium supplemented with 2% B27, 500 uM dbcAMP, 10 uM SB43152, 10 ng/mL BDNF, 10

ng/mL NT-3, 1 uM Ken, 2 mM Glutamax-ITM and 1% penicillin/streptomycin), half of the medium was changed every 2 days.

The procedure for differentiation of miNSCs is the same as for hiNSCs.

Immunofluorescence staining

Cells were washed 3 times with PBS and then fixed with 4% paraformaldehyde (PFA, Sigma-Aldrich) for 10 min. Then cells were punched with 0.3% Triton for 10 min and blocked by 3% goat serum for 30 min at 37°C. After that, cells were incubated with primary antibodies overnight at 4°C followed by secondary antibody staining for 45 min at 37°C. After nuclear staining with Hoechst 33342 (Sigma-Aldrich), cells were observed and captured by Olympus CK51 microscope.

Flow cytometry

INSCs were dissociated using trypsin. Cell suspensions were first fixed with 4% formaldehyde for 10 mins on ice. After blocking for 30 min, cells were incubated with primary antibodies. After washing with PBS, cells were incubated with second antibodies. After another round of washing with PBS, FACS analysis was performed. Fluorochrome-matched isotype controls were used and subtracted during analysis.

In vivo assay

Three weeks wild-type nude mice were anesthetized with 5% chloral hydrate at 10 uL/g. Fix the anesthetized mice on the brain stereotaxic apparatus and fix the microinjector needle, subtract the brain fur with scissors, cut the brain skin with a scalpel, expose the mouse head, wipe with hydrogen peroxide, adjust the microinjector needle to the fontanelle of the mouse brain with its zero point. 2 uL P3 hiNSCs cell suspension (100k) was microinjected into one side of the telencephalon (x: -0.22 cm, y: -0.26 cm, z: -0.14 cm) for 3 min using a micro-syringe. After injection, the needle was held for 3 min and then slowly and gently pulled out for 3 minutes. 2 to 4 weeks after transplantation, the frozen section of the brain was analyzed with immunofluorescence.

MEA recording

For neuronal spontaneous action potential analysis on MEA plates, 24-well MEA plates containing 16 electrodes each were coated with 50 ug/mL laminin for three h at 37°C. The neurons derived from the differentiation of iNSCs were digested and centrifuged, the supernatant was removed, the amount of cell culture medium (neural induction media as previously described) added was adjusted based on cell density, and the proper culture medium was added and mixed. 30 µL of the cell suspension to each pore was added to ensure that all drops apply to the electrodes for 1 h at 37°C (25,000 cells in a wall), then added 250 uL of culture medium was to each well, and then 259 µL of culture medium, changing the media by half every three days. DIV 9 to 21-day-old MEA cultures were used for analysis. 5 min recordings/1h were performed every day except the day of media change using an MEA system (Axion Biosystems). We set the action potential spike-detecting threshold to 5.5 standard deviations.

Cell Transplantation

In this study, 13.5-month-old male SAMP8 mice were used, purchased from the Animal Center of Peking University. GFP-labeled third-generation miR-302-hiNSCs were transplanted into the hippocampus's dentate gyrus (DG) region in SAMP8 mice, with the following relative coordinates to the anterior fontanelle: AP, -1.06 mm; ML, ± 1.0 mm; DV, -2.5 mm.

Behavioral tests

Behavioral tests were performed on SAMP8, SAMP8 with transplanted cells, and age-matched WT mice. Before the behavioral tests, the mice were placed in the laboratory for 30 minutes to adapt. The open field and novel object recognition tests were performed before the Y maze and Morris water maze tests. Thus, the order of the behavioral tests was: open field test, novel object recognition test, Y maze test, Morris water maze test, and running wheel test.

Open field test

The open field test setup consists of a white composite board measuring 40 cm in length, 40 cm in width, and 40 cm in height. The mice were placed in the center of the open field, each subject was placed in the same position, and a camera was fixed on top of the apparatus, recording the mouse's movements for 5 minutes. And the total distance, speed, and immobility time were recorded automatically using Ethovision XT16. The testing apparatus was wiped with clean paper towels containing 75% ethanol between the two mice being tested.

Novel object recognition test

On the first day, all mice were placed in the same equipment as the open field test to acclimate to the experimental environment in advance and were left alone to explore freely for 5 min. On the second day, two identical objects were placed in the apparatus, and each mouse was left to explore freely for 5 min. After 90 minutes, a new object was substituted for an old object, and the mice were allowed to explore for another 5 minutes, and the time spent exploring the old and new objects were recorded. The device was cleaned with 75% ethanol and wiped between the two subjects. The cognitive ability of the mice was tested by observing their exploration of old and new objects. The index observed was the new object recognition index, the time spent exploring new objects as T novel, exploring old objects as T old, and RI = T novel / (T novel + T old).

Y maze test

The Y-maze comprises three arms, with an angle of 120° between each arm. The size of each arm (length x width x height) is 10 cm x 5 cm x 5 cm. First, cover the novel arm with a barrier, place the mouse in the Y-maze for 5 minutes, then remove the mouse and return it to the cage for 1 hour. After 1 hour, remove the barrier from the novel arm, place the mouse from the starting arm, and let it freely move in the three arms

for 5 minutes. The spontaneous alternation rate is [(number of correct alternation responses) / (N-2)] × 100%.

Morris water maze test

The Morris water maze experiment includes a circular water pool with a diameter of 110 cm and height of 40 cm, a camera system, a platform, and a system for analyzing animal behavior trajectories. Starting from the first quadrant of the water pool, if the mouse reaches the platform within 60 seconds, it is allowed to stay on the platform for 10 seconds. If the mouse does not find the platform within 60 seconds, it is placed on it and allowed to stay for 10 seconds. The same procedure is repeated for the other three quadrants, and the mouse is dried with clean tissue after completing the test. The platform is hidden for the next five days, and the mouse undergoes training just like the first day, but with the platform hidden underwater. After six consecutive days of pre-training, the platform is removed, and the testing of the mouse begins. During the testing, the mouse is placed into the water from the opposite quadrant of the platform's original location and undergoes a 1-minute test. The video was recorded and analyzed using the Ethovision 16.0 software.

Wheel running test

For the running wheel experiment, the mouse is first acclimated to the running wheel for three days at a speed of 8 rpm. On day 4, an incremental protocol is used: the running wheel speed starts at 8 rpm and increases to 10 rpm after 2 minutes. Fatigue is defined as the mouse's unwillingness to move along the running wheel for at least 5 seconds despite mild electric shocks, and the distance and time of movement are recorded.

Fasting blood glucose measurement in mice

The tail tip of the mouse is gently pricked with a blood glucose needle, and the fasting blood glucose is measured with a blood glucose meter. During the fasting period, the mouse is allowed to drink water freely.

Body fat measurement

An instrument is used to measure the fat in the mouse to record the mass of lean tissue and fat.

Urine Urea Measurement

The urine urea concentration in the mouse is calculated using a urea assay kit (Elabscience).

Hair regrowth assay

On the first day, a 1×1 cm square of fur is shaved from the back of the mouse using a depilatory razor. Photos are taken after 14 and 28 days, and hair regrowth is evaluated using a 1–4 scale, with 4

representing complete hair regrowth, based on the photos and semi-quantitative assessment by two experimenters.

Statistical Analysis

In general, data for each result were obtained from 3 samples for cell culture and 8 animals for in vivo assay. Results are presented as the mean ± SD. Statistical analysis was performed using the Microsoft Excel computer programs and sigma 6.0. Unpaired two-tailed Student's-tests and/or Mann-Whitney U-test were used to perform the difference in RT-qPCR results. $P < 0.05$ was considered statistically significant.

Results

Single microRNAs rapidly and efficiently convert human and mouse fibroblasts into iNSCs

The current study aimed to explore the potential of a single miR-302a component of the miR-302/367 cluster in reprogramming human skin fibroblasts (HSF) into iNSCs. Previous literature has demonstrated the advantageous effects of combining the miR-302/367 cluster in improving the efficiency of reprogramming techniques [28, 29]. We created lentiviral/adenoviral vectors that encoded the miR-302a sequence, a member of the miR-302 cluster, and used them to convert human postnatal foreskin fibroblasts (HPFFs) obtained from postnatal sources to find out whether the overexpression of a single component of the miR-302 cluster can reprogram fibroblasts. Surprisingly, we discovered that simply overexpressing miR-302a converted HSF into NSCs quickly and efficiently. HPFFs (26- and 29-year-old males) and eyelid fibroblasts (41-year-old female) were isolated and identified as Vimentin positive and negative on Nestin, GFAP, and TUJ1 by immunostaining or RT-qPCR (Fig. S1).

The HPFFs, eyelid fibroblasts, and mouse cell line L929 cells were then infected with either a lentiviral or an adenovirus vector expressing miR-302a (Fig. 1A). For one day, we cultured HPFFs on gelatin-coated coverslips. Within 24 to 48 hours of miR-302a overexpression in HPFFs, their morphology changes rapidly, and clusters form. The earliest appearance of a colony was observed at 13 hours (Fig. 1B). To investigate the potential of miR-302a in reversing the aging phenotype, we hypothesized that miR-302a could substantially reverse the aging phenotype. After reprogramming for 1–2 days, we observed changes in the morphology of fibroblasts. Using optical microscopy, we observed that the cells formed colony structures and gradually became rounder with prolonged reprogramming. We quantified the morphological changes by calculating the ratio of "roundness" (maximum length divided by vertical width) of individual cells before, during, and after miR-302a reprogramming. Our results showed that successfully reprogrammed cells were significantly rounder and smaller in the middle stage of reprogramming compared to the initial fibroblasts, with significant differences (Fig. 1C-D). In contrast, negative control cells did not undergo substantial changes during miR-302a reprogramming and were significantly longer in the middle stage (Fig. 1C). The colony formation rate of HPFFs reached 1.11% three days after miR-302a the transfection, then grew to 2.29% on the fifth day and 8.92% on the seventh day. (Fig. 1E). Eyelid fibroblasts, like HPFFs, can form neurospheres rapidly and have a higher colony-

forming rate, Eyelid fibroblasts had a colony-forming rate of up to 3.04% on day 3 (Fig. S2), demonstrating that this approach to generating neurospheres from human fibroblasts is quicker and more effective than any currently existing method (Table S1).

Almost all of the transfected cells produced neurospheres within three days. The efficiency of the reprogramming can be improved by the addition of varying concentrations of VPA, VC, and polybrene. The ideal mixture of the three concentrations demonstrated a virus-cell transfection effectiveness of up to 90% using GFP-tagged transfected cells (Fig. 1F).

Immunostaining studies demonstrated that in the colonies, the levels of essential NSC biomarkers Nestin, OCT4, SOX2, and PAX6 were visible within 72 hours and subsequently increased over time with prolonged culture (Fig. 1G). On day 3, 90% of surviving infected fibroblasts were found to be Nestin positive by flow cytometry. These fibroblasts were reprogrammed into NSCs with a higher level of purity and quantity (Data not shown).

The induced neurospheres were harvested, broken down, and re-cultured in an NSC expansion medium for suspension and monolayer culture. Starting on day 2, the new iNSCs secondary neurospheres quickly developed. To enlarge and purify NSCs, suspension culture and monolayer culture are alternately used. For more than 10 months and more than 20 passes, the iNSCs could be expanded and maintained steadily. The morphologies of the iNSCs in passages 1, 2, 9, and 20 were uniform and stable (Fig. 1H), and they were uniformly positive for Nestin, SOX2, and PAX6 (Fig. 1I), demonstrating their capacity for self-renewal.

Zhang et al identified a cocktail of nine components that could efficiently reprogram identified mouse fibroblasts into a NSC-like cells using the percentage of SOX2+/Nestin + positive cells as a criterion for reprogramming efficiency [30]. INSCs expressed PAX6 Nestin and SOX2 markers in immunofluorescence and RT-qPCR results (Fig. 1I-K). The results of immunofluorescence strikingly confirmed the close similarity between hiNSCs and the control human Ptf1a-induced iNSCs (Fig. 1J and K). Based on the findings, we concluded that miR-302a transfected fibroblasts had a 90% reprogramming efficiency for NSCs. The transfection method with miR-302a for reprogramming fibroblasts into NSCs is faster and more effective than any other existing reprogramming method (Table S1). RT-qPCR analysis showed that the expression of Nestin, PAX6, and SOX2 in HPFFs undergoing reprogramming into NSCs started low on the first day and increased progressively over time (Fig. 1I). HiNSCs reprogrammed on glass slides expressed Nestin, PAX6, and SOX2 more strongly than cells connected directly to culture plates, and neurosphere development occurred more quickly. This outcome is quite comparable to that published by Bag óJR et al in 2017 [31]. OCT4 is not expressed during hiNSCs differentiation, hence the hiNSCs did not have a high OCT4 expression.

In an approach similar to HPFF reprogramming, mouse L929 cells were converted into NSCs utilizing miR-302a to demonstrate that they can reprogram both human and murine fibroblasts (Fig. S3A). 90% of the cells were spherical, clumped, and forming neurospheres by day 3. High levels of Nestin, SOX2, and PAX6 expression were seen in miR-302a-reprogrammed miNSCs from day 5 to day 11 (Fig. S3B and C).

The miNSCs expressed Nestin, SOX2, and PAX6 in a manner that was comparable to that of the SCR029 mouse cell line used as a control. The differentiation of miR-302a-reprogrammed mouse neural stem cells (miNSCs) into neurons, astrocytes, and oligodendrocytes was further studied both in vivo and in vitro. In vitro and in vivo, the miNSCs were differentiated into GFAP and Vimentin positive astrocytes, Olig2 and MBP positive oligodendrocytes, and MAP2 and TUJ1 positive neurons (Fig. S3D and E). Transplanted miNSCs were injected into adult mice's striatums and differentiated into astrocytes with GFAP and S100b immunoreactivity, or oligodendrocytes with Olig2 immunoreactivity, neurons with NeuN and TUJ1 immunoreactivity. (Fig. S4A-E). Quantification of the labeled cells in the sections revealed that, of the GFP + cells, 72.77%, 23.17%, 9.12%, 19.51%, and 22.27% differentiated into GFAP+, S100b+, Olig2+, NeuN+, and TUJ1 + cells derived from miNSCs (Fig. S4F). This technique for reprogramming mouse NSCs is quicker and more effective than currently used techniques, similar to the creation of human iNSCs (Table S2). These results demonstrate the effectiveness and efficiency of single miR-302a molecules in converting large quantities of human and mouse fibroblasts into iNSCs.

Multipotency of hiNSCs in vitro

The ability of iNSCs to produce oligodendrocytes, astrocytes, and neurons served as a measure of their developmental potential. INSCs were grown on feeders for three days to induce spontaneous differentiation. After the feeders, bFGF, and EGF were removed, the iNSCs differentiated into a significant proportion of TUJ1-positive neurons in four days. INSCs differentiated into neurons that were positive for TUJ1, MAP2, Nestin, SYN1, and NeuN after a further one to two weeks of culture (Fig. 2A and B). Three weeks later, a quantitative study revealed that 89% of the cells were TUJ1-positive (Fig. 2E). GFAP and Vimentin were both presents in the iNSC-derived astrocytes, according to immunocytochemistry (Fig. 2C). Additionally, during the differentiation process into oligodendrocytes, the hiNSCs were also able to differentiate into cells that were positive for MBP and Olig2 (Fig. 2D). 92% of the cells underwent astrocyte differentiation and became GFAP-positive astrocytes. 94% of developed cells in the oligodendrocyte differentiation media were MBP-positive (Fig. 2E). In iNSCs from various sources of fibroblasts, the expression patterns of the critical surface markers are comparable. These findings firmly establish the multipotency and ability of miR-302a-reprogrammed-iNSCs to generate a variety of neuronal subtypes.

The microelectrode array (MEA) analysis, a technique that measures the electrical activity of a cell population, was used to assess the electrophysiological function of neurons generated from iNSCs over a period of 9–21 days. The machine began recording spontaneous action potentials on day 9. The frequency of spontaneous action potentials gradually increased, peaked on day 21, and then began to decrease on day 22. Until cells die, this pattern will persist (Fig. 2F). The iNSC-derived neurons exhibit a distinctive spontaneous firing pattern in a synchronous cluster, demonstrating the maturation of the neural network. Differentiated cells display much more prominent and influential excitatory action potentials after stimulation (Fig. 2G, Fig. S6). Furthermore, cells expressing the synaptic protein synapsin can be observed during neuronal differentiation, indicating their ability to establish connections between

neurons (Fig. 2B). This demonstrates synaptic connections between the differentiated adult neurons. As a result, hiNSCs reprogrammed with miR-302a has the potential to develop into fully mature and functional neurons.

INSCs can survive, integrate and differentiate in mice brain in vivo.

The cortex and striatum of 3 to 5-week-old nude mice were microinjected with hiNSCs (Fig. 3; Fig. S5) and miNSCs (Fig. S4) to evaluate the in vivo developmental and differentiation capacity. Immunostaining showed that GFP-positive hiNSCs and miNSCs could be found and moved into the brain tissue adjacent to the implantation site after 2 to 4 weeks of transplantation. Transplanted hiNSCs and miNSCs could differentiate into neurons expressing TUJ1 and NeuN, generating astrocytes expressing GFAP and S100b and MBP and Olig2-positive glial cells (Fig. 3; Fig. S4, S5). The percentage of tagged cells in each region that differentiated into TUJ1+, NeuN+, GFAP+, S100b+, MBP+, and Olig2 + cells was 24.18%, 17.88%, 70.85%, 14.00%, 7.55%, and 7.20% (Fig. 3G). The transplantation of miR-302a-hiNSCs has successfully developed neurons, astrocytes, and oligodendrocytes within the mice's brains without causing any teratoma formation. Additionally, we examined many iNSCs from various passages; Hippocampal teratoma development was not observed. These findings suggest that miR-302a-hiNSCs can survive and develop in the adult brain in vivo and avoid teratoma development.

Anti-aging and antioxidant effects of culture supernatant from miR-302a-hiNSCs on senescent skin fibroblasts and NSCs

We investigated whether the supernatant of cultured miR-302a-hiNSC had anti-senescence and oxidative effects on HPFF. HPFF, SB431542-iPSC-iNSC, and miR-302a-hiNSC cultured with supernatant of HPFF, miR-302a-hiNSCs were treated with 300 mM hydrogen peroxide for 24 h. The supernatant of HPFF, SB-iPSC-iNSC, and miR-302a-hiNSC was treated with 300 mM hydrogen peroxide for 24 h. Compared to HPFF, SB-iPSC-iNSC Supernatant (SN), miR-302a-hiNSC SN consistently exhibited reduced senescence-associated β-galactosidase (β-gal) activity. Compared with H_2O_2 + HPFF, H_2O_2 + HPFF + miR-302a-hiNSCs SN exhibited reduced β-gal activity (Fig. 4A and B), reduced induced apoptotic cells, and increased cell proliferation (Fig. 4C and F). Using miR-302a-hiNSC conditioned media, fibroblasts exhibited a rounder cellular morphology, decreased cell volume, and fewer senescent cells were detected by staining (Fig. 4G and H). These results indicate that miR-302a can restore a youthful state in late-stage fibroblasts (P18). Next, we verified whether miR-302a-hiNSC itself has anti-aging and oxidative effects. Compared with miR-302a-hiNSC, SB-iPSC-iNSC, and H_2O_2-induced SB-iPSC-iNSC, H_2O_2-induced miR-302a-hiNSC consistently exhibited reduced senescence-associated β-galactosidase (β-gal) activity, with senescent cells reaching only 8.33%, while H_2O_2-induced SB-iPSC-iNSC senescent cells reached 46.67% (Fig. 4I and K). Compared with miR-302a-hiNSCs, H_2O_2-induced apoptotic cells of miR-302a-hiNSCs reached only 29.67% (Fig. 4J and L). Foxo3 regulates physiological oxidative stress response, Sirt6 overexpression delays aging, Nrf2 is a well-known transcription factor that regulates antioxidant expression, and we continued to investigate whether the three longevity factors Nrf2, Sirt6, and Foxo3 are expressed in miR-302a-hiNSCs.

We found that miR-302a-hiNSCs significantly increased the expression of Nrf2, Sirt6, and Foxo3 compared with control HPFF and Ptf1a-hiNSCs, and further expressed that miR-302a-hiNSCs could delay cellular senescence (Fig. 4M). MiR-302a-hiNSCs significantly improved the anti-aging and antioxidant capacity of fibroblasts. MiR-302a-hiNSCs significantly improved the expression of Nrf2, Sirt6 and Foxo3. Cells with significantly improved anti-aging and antioxidant capacity compared to supernatants cultured from iPSC-iNSCs sources.

MiR-302a-iNSCs improve spatial learning ability and memory in aged SAMP8 mice

We investigated the potential therapeutic benefits of miR-302a-hiNSC transplantation in the mouse SAMP8 model. At 4 and 8 weeks after miR-302a-hiNSCs were injected into the hippocampus of the SAMP8 mouse model, multiple tasks were carried out to assess the mice's cognitive health (14.5 and 15.5 months of age, respectively) (Fig. 5A). There were no differences in motor distance and motor speed between WT, SAMP8 and mice injected with miR-302a-hiNSCs in the 4w and 8w open-field experiments, while mice transplanted with miR-302a-hiNSCs spent less time at rest compared to WT and SAMP8 (Fig. 5C and F). There was no difference in the number of times, time and total percentage of correct spontaneous alternate responses (SAP) to explore the new foreign arm in the Y-maze test (Fig. 5D and G). The WT group and mice injected with miR-302a-hiNSCs spent more time examining new objects during the new object recognition test than the SAMP8 group (Fig. 5B and E), indicating that the SAMP8 mice injected with miR-302a-hiNSCs had a better short-term non-associative memory for the original environment.

We compared spatial learning and long-term memory between the three groups in the Morris water maze at 8 weeks post-transplantation (15.5 months of age). In all tests, we found significant differences in injected miR-302a-hiNSCs. SAMP8 mice showed latency deficits to find hidden platforms on days 5 and 6 of training compared to the WT group. At the same time point, mice injected with miR-302a-hiNSCs had a significantly lower mean escape latency than SAMP8 mice, indicating an improvement in spatial acquisition ability. Furthermore, mice injected with miR-302a-hiNSCs spent a longer time in the target quadrant and preferred the target platform location (Fig. 5H). These findings indicate that mice injected with miR-302a-hiNSCs have a strong memory for the previous location of the platform and improved spatial memory recovery. Finally, these findings show that injecting miR-302a-hiNSCs into the SAMP8 mouse model improves spatial learning and memory.

MiR-302a-hiNSCs regulate the expression of AD-related essential proteins in the SAMP8 mouse brain, restore endogenous neurons, and survive in the mouse brain for a long time

We used tissue immunofluorescence labeling analysis to measure the levels of various representative proteins in the hippocampus of three groups of mice to determine whether the increase in cognitive function in SAMP8 mice is accompanied by changes in crucial proteins in the brain. After transplantation of miR-302-hiNSCs for 120 days, GFP-positive transplanted cells were mainly located in the

hippocampus, projecting to the host dentate gyrus (DG) area (Fig. 6). The expression of AD-related p-Tau and Aβ was significantly reduced in the hippocampus. Compared with the SAMP8-PBS group, the content of AD-related Aβ (3.75 ± 0.75, n = 5) and p-Tau (3.296 ± 1.101, n = 5) proteins in SAMP8 mice transplanted with miR-302-hiNSCs was significantly reduced (Fig. 6A-D). To explore whether miR-302a-hiNSCs affect endogenous neurons, we analyzed SOX2 and Nestin proliferation markers in mouse coronal hippocampal slices. The results showed that the number of SOX2 (80.26 ± 7.681, n = 5) and Nestin (63.34 ± 5.036, n = 5) cells in the DG region of SAMP8 mice transplanted with miR-302-hiNSCs was significantly increased (Fig. 6E-H). In summary, these results suggest that miR-302a-hiNSCs regulate the expression of AD-related essential proteins, thus reducing neuronal damage and activating endogenous neurons, stabilizing the hippocampal neural network.

MiR-302a-hiNSCs improves health span, fat, weight, blood sugar, hair, fertility and hearing in aged SAMP8 Mice

To summarize the lifespan, we estimated the survival rate. At 50% survival, the median survival was 13 months for untreated male SAMP8 mice and 18.5 months for miR-302a-hiNSCs-treated SAMP8 mice. The SAMP8-miR-302a-hiNSCs-treated male mice exhibited a 37.8% extension in median lifespan, equivalent to a mean survival of 102.5 years, with significantly longer survival (Fig. 7A).

Physical activity is the primary criterion of the frailty index in elderly mice and has been clinically linked to human aging. Therefore, in this study, the running wheel experiment was chosen as the physical activity parameter to be compared between the two groups. The results showed that 16.5-month-old male SAMP8 mice had decreased physical activity, compared with same-month-old SAMP8-miR-302a-hiNSCs male mice that exercised longer distances on the running wheel and spent more time and turned the wheel on the running wheel (Fig. 7B). Thus, miR-302a-hiNSCs significantly improved the healthy lifespan of mice, promoted physical activity performance, and reduced frailty in old age.

To further explore the normoglycemic effect of miR-302a-hiNSCs transplantation on the organism, the blood glucose of mice in the SAMP8 and SAMP8-miR-302a-hiNSCs groups was measured after 12 hours of fasting and repeated once every other day for a total of three times. The outcomes demonstrated that the mice in the SAMP8 group had considerably higher blood glucose levels, while the blood glucose of the mice in the SAMP8-miR-302a-hiNSCs group was obviously lower than that of the SAMP8 mice, which was not significantly different from that of the mice in the WT group at the age of 50 years and was within the normoglycemic range (Fig. 7C). Thus, miR-302a-hiNSCs could improve the blood glucose of SAMP8 mice and maintain a relatively young level.

Next, we measured the body weight and adiposity parameters of the two groups of mice. The SAMP8-miR-302a-hiNSCs group had a higher body weight but were not statistically different from the SAMP8 mouse group. Regarding adiposity, the SAMP8-miR-302a-hiNSCs group differed substantially from the SAMP8 group (Fig. 7D and E).

The ability of hair regeneration diminishes with age. To investigate the effect of miR-302a-hiNSCs on hair growth, we shaved approximately 1 cm × 1 cm square of hair on the back of each mouse on the day of transplantation. At day 14, we observed that the back hair regeneration area of the mice in the transplantation group recovered to about 80%, and at day 28, the back hairs of miR-302a-hiNSCs transplantation-treated SAMP8 mice had completely regenerated the entire area. In contrast, the hair regeneration capacity of PBS-injected SAMP8 mice was much lower (Fig. 7F and G).

To evaluate the renal function of mice, we tested the urea concentration in the urine of two groups of mice at 17.5 months of age, and the urinary urea concentration of mice in the SAMP8-miR-302a-hiNSCs group was significantly lower compared to the SAMP8 group. Moreover, mice in the SAMP8-miR-302a-hiNSCs group could mate with females at 16.5 months of age (equivalent to 100 years of age in humans) and still had fertility (Fig. 7H and I). To explore the effect of transplanting miR-302a-hiNSC on the auditory function of SAMP8 mice, we selected three test frequencies (8 kHz, 16 kHz, and 32 kHz) as representatives of the low, mid and high-frequency regions of the cochlea, respectively. At the 8 kHz test frequency, the hearing threshold was 60 dB in SAMP8 mice and 35 dB in SAMP8 + miR-302a-hiNSC mice (Fig. S7A). At 16 kHz test frequency, the hearing threshold of SAMP8 mice was 55 dB and that of SAMP8 + miR-302a-hiNSC mice was 25 dB (Fig. S7B). At 32 kHz test frequency, the hearing threshold of SAMP8 mice was 45 dB, and the hearing threshold of SAMP8 + miR-302a-hiNSC mice was 25 dB (Fig. S7C). In conclusion, miR-302a-hiNSCs significantly prolonged the survival of SAMP8 mice, dramatically improved the healthy life span of mice, promoted physical activity performance, and improved the hair, fertility and hearing of SAMP8 mice.

Discussion

In this study, we demonstrate the use of a unique miR-302a reprogramming-based source of induced NSCs that promote cognitive improvement, life extension, and physical function in a murine model of late-stage severe AD. An Important feature of this cell is that it expresses Nrf2, Sirt6 and Foxo3 in addition to the fundamental NSC signatures. Both human and murine fibroblasts can be employed to efficiently and rapidly establish iNSCs cells in about 2–3 days, and in vitro and in vivo studies have been performed to determine their function. These results support that autologous cell reprogramming into NSC technology can be a viable approach to conventional autologous therapy without the necessity for invasive brain biopsies or lifelong immunosuppressive therapy.

We plan to apply next-generation cell reprogramming technology to generate highly efficient and quickly accessible autologous-induced NSCs for treating neurodegenerative illnesses. In a clinical environment, autologous cells' ability to tolerate immune rejection may provide more significant therapeutic results than allogeneic NSCs therapies now being investigated in clinical trials.

HiNSC can differentiate into different types of neural cells, providing a potential source for repairing degenerated or damaged brains. However, human adult NSCs persist in the brain while encountering continuous challenges from age or injury-related changes in the brain environment (e.g., oxidative stress),

gradually decreasing or depleting and becoming increasingly less functional. Aging is linked to cognitive loss and the emergence of numerous diseases such as Alzheimer's, Parkinson's, aging, and cancers [9, 32, 33]. Therefore, the in vitro culture of human-induced neural stem/progenitor cells and their possible therapeutic applications have received particular attention [27].

In recent years, direct reprogramming techniques have been used to generate NPCs from murine and human somatic cells, which resemble NSCs in the brain [34]. The reprogramming of iNSCs using techniques that involve pluripotent transcription factors like SOX2 or OCT4 and non-neural pluripotent transcription factors like BMi1, Zfp521, and Ptf1a faces issues including low induction efficiency and a lengthy process [21–26, 29, 35, 36]. We use a single miR-302a reprogrammed fibroblast into direct iNSCs. In this single step, the rapid generation of large numbers of transplantable cells is critical for the cure of disease, as patients with severe degenerative disease or tumors often have little time left to live [37]. In addition, the direct reprogramming process can eliminate the potential tumorigenicity of the iPS stage and help ensure that iNSCs do not form tumors in vivo. To further maximize the clinical translation potential of our study, we employed a single reprogramming strategy of miR-302a, which can substantially increase the generation rate of hiNSCs using microRNAs compared to existing reprogramming methods [38].

It is a new observation. Some studies have shown that miR-302 clusters can combine miR-367 to reprogram somatic cells into IPS with high efficiency [38]. However, none of the studies showed that using a miR-302a alone can perform reprogramming somatic cells into NSCs. We determined that miR-302a alone can efficiently and rapidly reprogram fibroblasts into NSCs based on miR-302 cluster reprogramming. In vivo and in vitro cultures, hiNSCs can differentiate into both glial cells and neurons and does not express pluripotency markers. In vivo, hiNSCs survives for more than four weeks and remains positive for Nestin or TUJ1, but does not express OCT4. The fibroblasts utilized in this study were sourced from the patient's skin and are subject to aging in parallel with the body. Research has demonstrated that the proliferative capacity of fibroblasts gradually diminishes during continuous passages, displaying aging characteristics during in vitro continuous passages. Moreover, it has been verified that the proliferation potential of late passage (P21) cells decreases significantly and exhibits apparent aging characteristics [39]. The direct conversion of skin fibroblasts obtained from elderly individuals into iNSCs has long been challenging [40]. As numerous reports suggest that the efficiency of reprogramming somatic cells from aged sources to stem cells is lower compared to young or neonatal cells [41–43]. Research has demonstrated a negative correlation between donor age and reprogramming efficiency in transfected transcription factor cells [44, 45]. Reprogramming efficiency is positively correlated with cell proliferation and negatively associated with cell aging. Based on these early observations, it was found that the overexpression of hSOX2 or the use of M9 compounds could not effectively reprogram skin fibroblasts from 55-75-year-old individuals into iNSCs [29, 30]. When these two methods were combined, the efficiency of reprogramming fibroblasts into iNSCs was relatively low (0.038–0.091%). This inefficiency is mainly because the fibroblasts used in the study were older than the embryonic dermal cells used in the original paper [44]. Numerous studies have shown that transfection efficiency is high in 3–5 passage fibroblasts [45, 46]. However, research rarely involves reprogramming

middle-to-late passage fibroblasts from elderly sources into anti-aging iNSCs. However, our study indicates that a single miR-302a reprogramming strategy can effectively and rapidly convert P18 passage-aged HSF into iNSCs with mature neuronal features within 2–3 days. The analysis of cell surface markers and molecular and functional assays have confirmed this. Furthermore, the efficiency of this method is remarkably high, with a transfection rate exceeding 90% and a clone formation rate of 3%, far surpassing the current international conversion efficiency standards.

Previous studies have shown that transcriptomic and epigenetic changes are reversible in principle. Fibroblasts undergo a mesenchymal to epithelial-like transition in cell morphology after 10–17 days of reprogramming and gradually form colony structures that become larger with longer reprogramming [47]. However, our study found that the morphology of fibroblasts changed after 1–2 days of cell reprogramming, with successfully reprogrammed cells becoming significantly rounder, more minor, and proliferating faster in the intermediate stages of reprogramming. Our results found that aged-derived HPFF (P18) can be efficiently and rapidly reprogrammed to rejuvenate iNSC in the presence of miR-302a. It has been shown that cell size increases during human fibroblast senescence. Senescence in human cell lines is associated with significant changes in cell size, and senescent cells become very large in morphology and volume, which in turn selectively lose haploid genes, limit cell growth and proliferation, and display phenotypic characteristics of senescent cells, including slow cell division and increased DNA damage [48]. However, we found human senescent fibroblasts in the 18th generation d after treatment with miR-302a-hiNSCs supernatant for 24 h. The cell cytosol became elliptical, smaller, and more elongated in size, and less senescent cells were found by β-galactosidase staining, and the cells became younger. The results suggest that miR-302a-hiNSCs can rapidly rejuvenate late-stage fibroblasts (P18). Moreover, this NSC expresses Nrf2, Sirt6, and Foxo3, which have antioxidant and anti-aging properties, and the potential therapeutic use of the resulting human iNSC remains to be explored.

The most common form of dementia, AD, is now incurable [49]. The pathological features of AD include progressive accumulation of amyloid-β (Aβ) protein, tau-rich neurofibrillary tangles, widespread synaptic damage, and neuronal loss in the brain of patients. Treatment for AD currently only addresses symptoms and medication, with no ability to slow disease progression. Several promising treatments targeting Aβ or tau failed to improve cognitive impairment in AD patients in recent clinical studies. Stem cell therapy has emerged as a possible treatment option for neurological illnesses. Many animal studies demonstrated that mesenchymal stem cells (MSCs), induced pluripotent stem cells (iPS), or NSCs have a positive role in AD treatment and may improve cognitive performance through a variety of immunological, histological, and genetic measures [15, 27, 50–54]. However, MSCs suffer from immune rejection and are not yet able to differentiate into corresponding neural cells and build neural connections at the damaged site, which affects their long-lasting effects. In contrast, autologous-induced NSCs do not have these problems and can also differentiate to form neurons. Functional integration of iNPC-derived neurons with host synaptic networks improves hippocampal plasticity and neural circuit repair in the host brain, resulting in improved cognitive function in AD mice [27]. As NSCs repair capacity is limited in vivo, in vitro NSC supplementation can replenish NSC stocks to repair neurons lost after disease or injury.

Efforts to convert human somatic cells into iNSCs for cell replacement therapy have been extensive. In our study, we characterized the iNSCs generated through miR-302a and evaluated their effectiveness in an animal model of late-onset AD. Studies have shown that AD is primarily a sporadic, late-onset disease with an exponential increase in prevalence starting at age 65. The SAMP8 mouse has several distinct benefits over genetically modified models, and it is especially well adapted to studying the "transition" from aging to AD. The SAMP8 mouse phenotype reflects the symptoms of humans with late-onset and aging-related sporadic AD [55]. Previous studies have shown that transplantation of clinical-grade human umbilical cord-derived Mesenchymal stem cells improves cognitive function, downregulates phosphorylated tau, and attenuates neuronal damage in 4-month-old male SAMP8 mice [15]. As a result, we used 13.5-month-old SAMP8 mice as an animal model of late AD in our study, which is similar to 85 years in people. We transplanted human iNSCs into the hippocampus region. We found significant increases in dependent learning and memory abilities in three behavioral tests (open field experiment, Y-maze, and Morris water maze) four and eight weeks later. We show that miR-302a-hiNSCs can restore cognitive capacity in SAMP8 mice, an aging accelerated AD mouse model. We show that miR-302a-hiNSCs regulate the expression of AD-related critical proteins in the brains of SAMP8 mice, including downregulation of hyperphosphorylated tau, improvement of neurofibrillary tangles, restoration of endogenous neurons, and long-term survival in the mouse brain, promoting synaptic plasticity in the aged hippocampus, all of which are linked to memory impairment.

Most diseases that impact the elderly population are primarily attributed to the aging process. Research suggests that various biological processes, including oxidative stress, telomere depletion, cellular depletion, and cellular senescence, play a role in age-related diseases [56]. The decline in the number or deficit of NSCs significantly contributes to systemic aging [12]. As a result, stem cell transplantation, exosome injection, anti-oxidative stress strategies, and telomere supplementation have been proposed to delay aging by supplementing or activating the relevant stem cells [12, 16, 57]. Although stem cell transplantation can prolong life, the benefit is brief and requires the use of young stem cells [12]. Exosomes must be injected multiple times, and the exosomes required are also derived from young stem cells. Older exosomes are useless, and exosome injections no longer work once the organism reaches a certain age [16].

Given this backdrop, the impact of miR-302a-derived iNSCs on senescence-affected tissues in rapidly aging mice remains to be explored. The present study aims to fill this knowledge gap by demonstrating that miR-302a-iNSCs have substantial anti-aging potential and that in vitro cellular experiments have shown that iNSCs to have more vital antioxidant and anti-aging effects than normal NSCs.

Sirt6 has antioxidant effects, and overexpression of Sirt6 alone can extend the life span by 30% [58]. Nrf2 and Sirt6 can be combined to promote the antioxidant effect of stem cells [59]. According to a study, Sirt6 can extend the median lifespan of fruit flies by 33–38% [60]. A more robust Sirt6 activity means a longer lifespan [61]. Reshaping energy balance can extend the lifespan of mice by 30% by targeting Sirt6, which has an essential regulatory function in fat metabolism [58]. Studies have showed that Sirt6 is vital in promoting fat-burning and regulating liver fat metabolism [62]. Our experiment also proved that miR-

302a-hiNSC expressing Sirt6 could prolong lifespan and promote regulation of fat metabolism, which is similar to the results of the two articles mentioned above. In addition, Bazhen Yimu Wan can promote hippocampal Sirt6 expression, improve oxidative damage, delay aging, and promote exercise capacity enhancement and fur regeneration [63], similar to the experimental results of our transplantation of miR-302a-hiNSC. However, we only need one transplantation and do not need long-term transplantation, so the effect is better. In 2016, Guanghui Liu et al conducted a protective study on mesenchymal stem cells expressing Sirt6 and found that it can activate antioxidant gene expression and participate in maintaining human stem cell homeostasis with Nrf2 [59], which is similar to our experimental results of iNSC expressing Sirt6 and Nrf2, prolonging lifespan and promoting maintenance of iNSC homeostasis in the hippocampus.

Because Nrf2 has an antioxidant effect, it can promote the survival of NSCs and the life-prolonging effect of the organism [64–67], Studies have shown that drinking coffee can extend life expectancy by 24% because coffee contains chlorogenic acid, which can activate the Nrf2 signaling pathway [68]. At low concentrations, metformin can extend the lifespan of worms by 40% and mice by 10.3%. In addition to activating the AMPK signaling pathway, the Nrf2 signaling pathway must be activated to extend lifespan [68, 69]. Liu Guanghui et al used gene editing technology to rewrite a single nucleotide in exon 2 of the Nrf2 coding gene in the human genome genetic code. They used single-nucleotide Nrf2 genetic enhancement MSC to obtain genetically enhanced "super" stem cells (Genetically Enhanced Stem cells, GES cells) for the first time in the laboratory. These GES cells have dual resistance to cell aging and tumorigenic transformation, providing a possible solution for safe and effective stem cell therapy [70]. Our miR-302a-hiNSCs also express Nrf2, which can be regarded as a genetically enhanced version of iNSCs similar to Nrf2. The median survival of SAMP8 male mice transplanted with miR-302a-hiNSCs increased from 12.8 months to 18 months, representing a 40.625% life extension. And they can also anti-aging, resist oxidative stress, and even resist tumorigenic malignant transformation. Therefore, iNSCs constructed by miR-302a also provide a practical solution for us to carry out safe and effective stem cell therapy.

Foxo3 also has an important role in stress resistance in NSCs [32]. Studies have shown that Foxo3 can protect NSCs from stress stimulation, thereby ensuring the long-term stable existence of NSCs [32]. This study may help explain why specific Foxo3 versions are associated with exceptionally long and healthy lifespans—they may help maintain reasonable NSPC reserves. Guanghui Liu and Jing Qu et al used gene editing to obtain high-quality human vascular cells that can delay aging, resist external stress, enhance vascular homeostasis, and resist malignant transformation induced by oncogenes, providing a safer clinical treatment strategy and solution [17]. Our results show that Foxo3 is also expressed in miR-302a-hiNSCs, so these cells can protect cells from stress stimulation to maintain reasonable NSC reserves. Compared with mesenchymal stem cell transplantation for treating AD, animal models and hypothalamic anti-inflammatory NSC transplantation, transplanted cells for two months to detect cell survival and expression of related markers. The study used young mesenchymal stem cells, strictly limited to P3-P5 generations [15]. We used P18 fibroblasts to reprogram iNSCs for transplantation, which can be passaged over 20 generations. P2, P9 and P20 were tested to have similar phenotypic and functional

status.Previous studies have shown that transplantation of NSCs can extend life by 10% in 8-month-old mice, equivalent to transplantation in humans at about 35 years of age. All in all, this experiment was implanted in SAMP8 mice transplanted at 13.5 months, equal to 85 years of age in humans, with a 40.625% life extension to a median survival of 18 months, which corresponds to an average survival of 105.88 years. The 40.625% life-extension result obtained with iNSCs was much higher than the 10% life-extension result obtained with anti-inflammatory NSCs. This result may be related to the expression of Nrf2, Sirt6, and Foxo3 by these iNSCs.

In the study of hypothalamic NSC longevity, they used IkBα-htNSCs anti-inflammatory NSCs because normal NSCs have a poor survival rate in vivo due to inflammatory environmental stress and immune rejection and almost disappear after two months. However, IkBα-htNSC anti-inflammatory NSCs can remain at about 50% after two months. Since cell survival is only 2–3 months, the longevity effect cannot be explained by neural cells. They turned to miRNA and found that injecting microRNA-rich exosomes isolated from young hypothalamic stem cell cultures into mice can delay the decline of the animal body and cognitive function. Its effect is almost equivalent to that of stem cell injection [12]. Our results showed that after transplantation for four months, the GFP miR-302a-hiNSCs not only survived but also existed in large quantities and differentiated into neurons. The results showed that miR-302a-hiNSCs expressing Nrf2 and Foxo3 could resist inflammatory environment and stress after transplantation and continue to function normally for four months, thus promoting longevity. In addition, no tumor formation was found. Therefore, it is the cells themselves that play a role. Moreover, we used miR-302a transfection-induced reprogrammed NSCs. MiR-302a-induced iNSCs can prolong life, resist stress environment, maintain cell homeostasis, and resist malignant transformation induced by oncogenes. The construction and application of miR-302a-hiNSC cells provide a safer clinical treatment strategy and solution.

Studies have shown that the brain and testes have significant similarities and can share 92% of similar proteins, including Nestin. Its expression pattern is similar, decreasing with age [71]. As aging progresses, the expression of Nestin and other proteins in testicular stromal cells decreases, leading to decreased testosterone secretion, decreased sperm production ability, and reproductive aging. After melatonin treatment, Nestin expression can be increased, testosterone secretion restored, and sperm production promoted, thereby restoring reproductive ability [72]. Our results show that after iNSC transplantation, some nestin-positive cells still exist in the hippocampus, indicating that some iNSCs have established a stable iNSC cell bank in the hippocampus. It will produce nestin protein, which may circulate throughout the body with body fluids. In mice transplanted with iNSCs, at an age equivalent to 100 years old, SAMP8 mice produced four pups with young female mice and cages, indicating that they can produce sperm, while the control group without transplanted cells did not produce pups. This result may indicate that after iNSC transplantation, undifferentiated iNSCs continue to produce Nestin protein, which may be transported to the testes with body fluids, increasing nestin expression in the testes, promoting testosterone secretion, promoting sperm production, and leading to restored reproductive ability.

Regarding physical strength index, the ageing SAMP8 mice transplanted with iNSCs were no worse than the young mice. Aging male SAMP8 mice transplanted with iNSCs ran farther on the running wheel,

exercised longer, and were more resistant to fatigue than control SAMP8 mice. We found that hiNSCs transplantation improved the deterioration of blood glucose due to aging and better-maintained serum glucose levels and energy homeostasis. This result is similar to that sirt6 overexpressing mice can restore blood glucose and energy homeostasis [58]. The results suggest that Sirt6 expressed in iNSCs may be involved in glycemic regulation and energy homeostasis. It was found that iNSCs transplantation improved the increase in adiposity due to aging in SAMP8 mice and better maintained adipose homeostasis. This result also suggests that Sirt6 expressed in iNSCs may be involved in the regulation of lipid homeostasis. It is crucial to note that when we assessed renal performance based on urinary urea concentration, this could be a result of the decreased skeletal muscle catabolic rate and the change in urea content, indicating a considerable improvement in renal function. Additionally, we carried out mating studies on 16.5-month-old SAMP8, and we discovered that while no mice were born in the SAMP8-only group, four mice were born in the SAMP8 group transplanted with iNSCs. The outcomes showed that at the equivalent of 100 years in human life, the SAMP8 mice implanted with iNSCs were still capable of reproducing normally. Other experiments have not revealed anything similar.

Conclusion

Our study highlights the potential of iNSCs generated based on miR-302a as a promising therapeutic approach for treating various age-related diseases and conditions. We found the iNSCs treatment to improve lifespan, cognitive abilities in late-stage AD, fatigue resistance, hair regeneration, blood glucose, and fat metabolism, renal function, reproductive function, and hearing loss. Further research will compare iNSCs from patient versus control donors, isolation and purification of iNSCs exosomes and optimisation of therapeutic pathways. These results pave the way for a novel approach to the rapid and efficient production of antioxidant and anti-aging hiNSCs for the preservation of cognitive function, improvement of aging, and prolongation of lifespan in AD patients.

Declarations

Supplementary Information

Supporting Information is available from the author.

Acknowledgments

We thank Ruonan Li for animal feeding, Renhui Zhan for RT-qPCR, Yanwei Wang for primary cell collection from human foreskin, Xuemei Hu for partial financial support and advice, Bo Dai for primary cell collection from human Eyelid and some writing advice, Yeying Sun for human IPS. The authors would like to thank Prof. Mengqing Xiang and Dr. Dongchang Xiao (Sun Yat-sen University) for providing the human and murine NSCs.

Authors contributions

Z. conducted the animal experiments, sample collection and measurement. Y.L. and J.S. helped with the sample collection. Y.Z., Y.L. and J.S. conducted data analysis. Y.Z. and T.X. conducted the electrophysiological experiments. Y.W. and Y.Z. collaborated on writing and refining the manuscript. Y.W. conceived and supervised the study, provided funding and finalized the manuscript. All authors have reviewed the manuscript and approved the submission.

Funding

This work was supported by the Shandong Province Natural Science Foundation Grants ZR2018LC008 (Y.W.) and Yantai Science and Technology Innovation Development Plan 2020XDRH106 (Y.W.).

Availability of data and materials

Correspondence and request for data or materials should be addressed to Yuesi Wang.

Ethics approval and consent to participate

All experiments with animals were approved by the Ethics Committee of Binzhou Medical University.

Consent for publication

Not applicable

Competing interests

Authors declare that they have no competing interests.

References

1. Rando TA, Wyss-Coray T. Asynchronous, contagious and digital aging. Nat Aging. 2021;1(1):29-35.
2. Kennedy BK, Berger SL, Brunet A, Campisi J, Cuervo AM, Epel ES, et al. Geroscience: linking aging to chronic disease. Cell. 2014;159(4):709-13.
3. Hou Y, Dan X, Babbar M, Wei Y, Hasselbalch SG, Croteau DL, et al. Ageing as a risk factor for neurodegenerative disease. Nat Rev Neurol. 2019;15(10):565-81.
4. Hao ZZ, Wei JR, Xiao D, Liu R, Xu N, Tang L, et al. Single-cell transcriptomics of adult macaque hippocampus reveals neural precursor cell populations. Nat Neurosci. 2022;25(6):805-17.
5. Kalamakis G, Brüne D, Ravichandran S, Bolz J, Fan W, Ziebell F, et al. Quiescence Modulates Stem Cell Maintenance and Regenerative Capacity in the Aging Brain. Cell. 2019;176(6):1407-19.e14.
6. Moreno-Jiménez EP, Flor-García M, Terreros-Roncal J, Rábano A, Cafini F, Pallas-Bazarra N, et al. Adult hippocampal neurogenesis is abundant in neurologically healthy subjects and drops sharply in patients with Alzheimer's disease. Nat Med. 2019;25(4):554-60.

7. Gontier G, Iyer M, Shea JM, Bieri G, Wheatley EG, Ramalho-Santos M, et al. Tet2 Rescues Age-Related Regenerative Decline and Enhances Cognitive Function in the Adult Mouse Brain. Cell Rep. 2018;22(8):1974-81.
8. Ibrayeva A, Bay M, Pu E, Jörg DJ, Peng L, Jun H, et al. Early stem cell aging in the mature brain. Cell Stem Cell. 2021;28(5):955-66.e7.
9. Navarro Negredo P, Yeo RW, Brunet A. Aging and Rejuvenation of Neural Stem Cells and Their Niches. Cell Stem Cell. 2020;27(2):202-23.
10. Urbán N, Blomfield IM, Guillemot F. Quiescence of Adult Mammalian Neural Stem Cells: A Highly Regulated Rest. Neuron. 2019;104(5):834-48.
11. Bast L, Calzolari F, Strasser MK, Hasenauer J, Theis FJ, Ninkovic J, et al. Increasing Neural Stem Cell Division Asymmetry and Quiescence Are Predicted to Contribute to the Age-Related Decline in Neurogenesis. Cell Rep. 2018;25(12):3231-40.e8.
12. Zhang Y, Kim MS, Jia B, Yan J, Zuniga-Hertz JP, Han C, et al. Hypothalamic stem cells control ageing speed partly through exosomal miRNAs. Nature. 2017;548(7665):52-7.
13. Yang JH, Hayano M, Griffin PT, Amorim JA, Bonkowski MS, Apostolides JK, et al. Loss of epigenetic information as a cause of mammalian aging. Cell. 2023;186(2):305-26.e27.
14. Schultz MB, Sinclair DA. When stem cells grow old: phenotypes and mechanisms of stem cell aging. Development. 2016;143(1):3-14.
15. Jia Y, Cao N, Zhai J, Zeng Q, Zheng P, Su R, et al. HGF Mediates Clinical-Grade Human Umbilical Cord-Derived Mesenchymal Stem Cells Improved Functional Recovery in a Senescence-Accelerated Mouse Model of Alzheimer's Disease. Adv Sci (Weinh). 2020;7(17):1903809.
16. Sanz-Ros J, Romero-García N, Mas-Bargues C, Monleón D, Gordevicius J, Brooke RT, et al. Small extracellular vesicles from young adipose-derived stem cells prevent frailty, improve health span, and decrease epigenetic age in old mice. Sci Adv. 2022;8(42):eabq2226.
17. Yan P, Li Q, Wang L, Lu P, Suzuki K, Liu Z, et al. FOXO3-Engineered Human ESC-Derived Vascular Cells Promote Vascular Protection and Regeneration. Cell Stem Cell. 2019;24(3):447-61.e8.
18. Vierbuchen T, Wernig M. Direct lineage conversions: unnatural but useful? Nat Biotechnol. 2011;29(10):892-907.
19. Okano H, Nakamura M, Yoshida K, Okada Y, Tsuji O, Nori S, et al. Steps toward safe cell therapy using induced pluripotent stem cells. Circ Res. 2013;112(3):523-33.
20. Kelaini S, Cochrane A, Margariti A. Direct reprogramming of adult cells: avoiding the pluripotent state. Stem Cells Cloning. 2014;7:19-29.
21. Kim YJ, Lim H, Li Z, Oh Y, Kovlyagina I, Choi IY, et al. Generation of multipotent induced neural crest by direct reprogramming of human postnatal fibroblasts with a single transcription factor. Cell Stem Cell. 2014;15(4):497-506.
22. Mitchell RR, Szabo E, Benoit YD, Case DT, Mechael R, Alamilla J, et al. Activation of neural cell fate programs toward direct conversion of adult human fibroblasts into tri-potent neural progenitors using

OCT-4. Stem Cells Dev. 2014;23(16):1937-46.

23. Moon JH, Heo JS, Kim JS, Jun EK, Lee JH, Kim A, et al. Reprogramming fibroblasts into induced pluripotent stem cells with Bmi1. Cell Res. 2011;21(9):1305-15.
24. Shahbazi E, Moradi S, Nemati S, Satarian L, Basiri M, Gourabi H, et al. Conversion of Human Fibroblasts to Stably Self-Renewing Neural Stem Cells with a Single Zinc-Finger Transcription Factor. Stem Cell Reports. 2016;6(4):539-51.
25. Thier M, Worsdorfer P, Lakes YB, Gorris R, Herms S, Opitz T, et al. Direct conversion of fibroblasts into stably expandable neural stem cells. Cell Stem Cell. 2012;10(4):473-9.
26. Xiao D, Liu X, Zhang M, Zou M, Deng Q, Sun D, et al. Direct reprogramming of fibroblasts into neural stem cells by single non-neural progenitor transcription factor Ptf1a. Nature Commun. 2018;9(1):2865.
27. Zhang T, Ke W, Zhou X, Qian Y, Feng S, Wang R, et al. Human Neural Stem Cells Reinforce Hippocampal Synaptic Network and Rescue Cognitive Deficits in a Mouse Model of Alzheimer's Disease. Stem Cell Reports. 2019;13(6):1022-37.
28. Mertens J, Marchetto MC, Bardy C, Gage FH. Evaluating cell reprogramming, differentiation and conversion technologies in neuroscience. Nature Rev Neurosci. 2016;17(7):424-37.
29. Ring KL, Tong LM, Balestra ME, Javier R, Andrews-Zwilling Y, Li G, et al. Direct reprogramming of mouse and human fibroblasts into multipotent neural stem cells with a single factor. Cell Stem Cell. 2012;11(1):100-9.
30. Zhang M, Lin YH, Sun YJ, Zhu S, Zheng J, Liu K, et al. Pharmacological Reprogramming of Fibroblasts into Neural Stem Cells by Signaling-Directed Transcriptional Activation. Cell Stem Cell. 2016;18(5):653-67.
31. Bagó JR, Okolie O, Dumitru R, Ewend MG, Parker JS, Werff RV, et al. Tumor-homing cytotoxic human induced neural stem cells for cancer therapy. Sci Transl Med. 2017;9(375).
32. Hwang I, Uchida H, Dai Z, Li F, Sanchez T, Locasale JW, et al. Cellular stress signaling activates type-I IFN response through FOXO3-regulated lamin posttranslational modification. Nat Commun. 2021;12(1):640.
33. Bin Imtiaz MK, Jaeger BN, Bottes S, Machado RAC, Vidmar M, Moore DL, et al. Declining lamin B1 expression mediates age-dependent decreases of hippocampal stem cell activity. Cell Stem Cell. 2021;28(5):967-77.e8.
34. Brand AH, Livesey FJ. Neural stem cell biology in vertebrates and invertebrates: more alike than different? Neuron. 2011;70(4):719-29.
35. Fang L, El Wazan L, Tan C, Nguyen T, Hung SSC, Hewitt AW, et al. Potentials of Cellular Reprogramming as a Novel Strategy for Neuroregeneration. Front Cell Neurosci. 2018;12:460.
36. Zou Q, Yan Q, Zhong J, Wang K, Sun H, Yi X, et al. Direct conversion of human fibroblasts into neuronal restricted progenitors. J Biol Chem. 2014;289(8):5250-60.

37. Stupp R, Hegi ME, Mason WP, van den Bent MJ, Taphoorn MJ, Janzer RC, et al. Effects of radiotherapy with concomitant and adjuvant temozolomide versus radiotherapy alone on survival in glioblastoma in a randomised phase III study: 5-year analysis of the EORTC-NCIC trial. Lancet Oncol. 2009;10(5):459-66.
38. Anokye-Danso F, Trivedi CM, Juhr D, Gupta M, Cui Z, Tian Y, et al. Highly efficient miRNA-mediated reprogramming of mouse and human somatic cells to pluripotency. Cell Stem Cell. 2011;8(4):376-88.
39. Meng Q, Gao J, Zhu H, He H, Lu Z, Hong M, et al. The proteomic study of serially passaged human skin fibroblast cells uncovers down-regulation of the chromosome condensin complex proteins involved in replicative senescence. Res Commun. 2018;505(4):1112-20.
40. Rocchi A, Orsucci D, Tognoni G, Ceravolo R, Siciliano G. The role of vascular factors in late-onset sporadic Alzheimer's disease. Genetic and molecular aspects. Curr Alzheimer Res. 2009;6(3):224-37.
41. Cheng Z, Ito S, Nishio N, Xiao H, Zhang R, Suzuki H, et al. Establishment of induced pluripotent stem cells from aged mice using bone marrow-derived myeloid cells. J Mol Cell Biol. 2011;3(2):91-8.
42. Li H, Collado M, Villasante A, Strati K, Ortega S, Cañamero M, et al. The Ink4/Arf locus is a barrier for iPS cell reprogramming. Nature. 2009;460(7259):1136-9.
43. Ravaioli F, Bacalini MG, Franceschi C, Garagnani P. Age-Related Epigenetic Derangement upon Reprogramming and Differentiation of Cells from the Elderly. Genes. 2018;9(1).
44. Liu Y, Wang H. Modeling Sporadic Alzheimer's Disease by Efficient Direct Reprogramming of the Elderly Derived Disease Dermal Fibroblasts into Neural Stem Cells. J Alzheimers Dis. 2020;73(3):919-33.
45. Mahmoudi S, Mancini E, Xu L, Moore A, Jahanbani F, Hebestreit K, et al. Heterogeneity in old fibroblasts is linked to variability in reprogramming and wound healing. Nature. 2019;574(7779):553-8.
46. Hou PS, Chuang CY, Yeh CH, Chiang W, Liu HJ, Lin TN, et al. Direct Conversion of Human Fibroblasts into Neural Progenitors Using Transcription Factors Enriched in Human ESC-Derived Neural Progenitors. Stem Cell Reports. 2017;8(1):54-68.
47. Gill D, Parry A, Santos F, Okkenhaug H, Todd CD, Hernando-Herraez I, et al. Multi-omic rejuvenation of human cells by maturation phase transient reprogramming. eLife. 2022;11.
48. Neurohr GE, Terry RL, Lengefeld J, Bonney M, Brittingham GP, Moretto F, et al. Excessive Cell Growth Causes Cytoplasm Dilution And Contributes to Senescence. Cell. 2019;176(5):1083-97.e18.
49. Shi B, Zhao J, Xu Z, Chen C, Xu L, Xu C, et al. Chiral Nanoparticles Force Neural Stem Cell Differentiation to Alleviate Alzheimer's Disease. Adv sci (Weinh). 2022;9(29):e2202475.
50. Lee JK, Jin HK, Endo S, Schuchman EH, Carter JE, Bae JS. Intracerebral transplantation of bone marrow-derived mesenchymal stem cells reduces amyloid-beta deposition and rescues memory deficits in Alzheimer's disease mice by modulation of immune responses. Stem Cells. 2010;28(2):329-43.
51. Lee JK, Schuchman EH, Jin HK, Bae JS. Soluble CCL5 derived from bone marrow-derived mesenchymal stem cells and activated by amyloid β ameliorates Alzheimer's disease in mice by

recruiting bone marrow-induced microglia immune responses. Stem cells. 2012;30(7):1544-55.

52. Ma T, Gong K, Ao Q, Yan Y, Song B, Huang H, et al. Intracerebral transplantation of adipose-derived mesenchymal stem cells alternatively activates microglia and ameliorates neuropathological deficits in Alzheimer's disease mice. Cell Transplant. 2013;22 Suppl 1:S113-26.
53. Mendivil-Perez M, Soto-Mercado V, Guerra-Librero A, Fernandez-Gil BI, Florido J, Shen YQ, et al. Melatonin enhances neural stem cell differentiation and engraftment by increasing mitochondrial function. J Pineal Res. 2017;63(2).
54. Li Y, Li Y, Ji W, Lu Z, Liu L, Shi Y, et al. Positively Charged Polyprodrug Amphiphiles with Enhanced Drug Loading and Reactive Oxygen Species-Responsive Release Ability for Traceable Synergistic Therapy. J Am Chem Soc. 2018;140(11):4164-71.
55. Pallas M, Camins A, Smith MA, Perry G, Lee HG, Casadesus G. From aging to Alzheimer's disease: unveiling "the switch" with the senescence-accelerated mouse model (SAMP8). J Alzheimers Dis. 2008;15(4):615-24.
56. López-Otín C, Blasco MA, Partridge L, Serrano M, Kroemer G. The hallmarks of aging. Cell. 2013;153(6):1194-217.
57. Dorronsoro A, Santiago FE, Grassi D, Zhang T, Lai RC, McGowan SJ, et al. Mesenchymal stem cell-derived extracellular vesicles reduce senescence and extend health span in mouse models of aging. Aging Cell. 2021;20(4):e13337.
58. Roichman A, Elhanati S, Aon MA, Abramovich I, Di Francesco A, Shahar Y, et al. Restoration of energy homeostasis by SIRT6 extends healthy lifespan. Nat Commun. 2021;12(1):3208.
59. Pan H, Guan D, Liu X, Li J, Wang L, Wu J, et al. SIRT6 safeguards human mesenchymal stem cells from oxidative stress by coactivating NRF2. Cell Res. 2016;26(2):190-205.
60. Taylor JR, Wood JG, Mizerak E, Hinthorn S, Liu J, Finn M, et al. Sirt6 regulates lifespan in Drosophila melanogaster. Proc Natl Acad Sci U S A. 2022;119(5).
61. Tian X, Firsanov D, Zhang Z, Cheng Y, Luo L, Tombline G, et al. SIRT6 Is Responsible for More Efficient DNA Double-Strand Break Repair in Long-Lived Species. Cell. 2019;177(3):622-38.e22.
62. Naiman S, Huynh FK, Gil R, Glick Y, Shahar Y, Touitou N, et al. SIRT6 Promotes Hepatic Beta-Oxidation via Activation of PPARα. Cell Rep. 2019;29(12):4127-43.e8.
63. Li L, Zhang H, Chen B, Xia B, Zhu R, Liu Y, et al. BaZiBuShen alleviates cognitive deficits and regulates Sirt6/NRF2/HO-1 and Sirt6/P53-PGC-1α-TERT signaling pathways in aging mice. J Ethnopharmacol. 2022;282:114653.
64. Kubben N, Zhang W, Wang L, Voss TC, Yang J, Qu J, et al. Repression of the Antioxidant NRF2 Pathway in Premature Aging. Cell. 2016;165(6):1361-74.
65. Robledinos-Antón N, Rojo AI, Ferreiro E, Núñez Á, Krause KH, Jaquet V, et al. Transcription factor NRF2 controls the fate of neural stem cells in the subgranular zone of the hippocampus. Redox Bio. 2017;13:393-401.

66. Corenblum MJ, Ray S, Remley QW, Long M, Harder B, Zhang DD, et al. Reduced Nrf2 expression mediates the decline in neural stem cell function during a critical middle-age period. Aging Cell. 2016;15(4):725-36.
67. Anandhan A, Kirwan KR, Corenblum MJ, Madhavan L. Enhanced NRF2 expression mitigates the decline in neural stem cell function during aging. Aging Cell. 2021;20(6):e13385.
68. Siswanto FM, Sakuma R, Oguro A, Imaoka S. Chlorogenic Acid Activates Nrf2/SKN-1 and Prolongs the Lifespan of Caenorhabditis elegans via the Akt-FOXO3/DAF16a-DDB1 Pathway and Activation of DAF16f. The journals of gerontology Series A, A Biol Sci Med Sci. 2022;77(8):1503-16.
69. Martin-Montalvo A, Mercken EM, Mitchell SJ, Palacios HH, Mote PL, Scheibye-Knudsen M, et al. Metformin improves healthspan and lifespan in mice. Nat Commun. 2013;4:2192.
70. Yang J, Li J, Suzuki K, Liu X, Wu J, Zhang W, et al. Genetic enhancement in cultured human adult stem cells conferred by a single nucleotide recoding. Cell Res. 2017;27(9):1178-81.
71. Matos B, Publicover SJ, Castro LFC, Esteves PJ, Fardilha M. Brain and testis: more alike than previously thought? Open Biol. 2021;11(6):200322.
72. Yao S, Wei X, Deng W, Wang B, Cai J, Huang Y, et al. Nestin-dependent mitochondria-ER contacts define stem Leydig cell differentiation to attenuate male reproductive ageing. Nat Commun. 2022;13(1):4020.

Figures

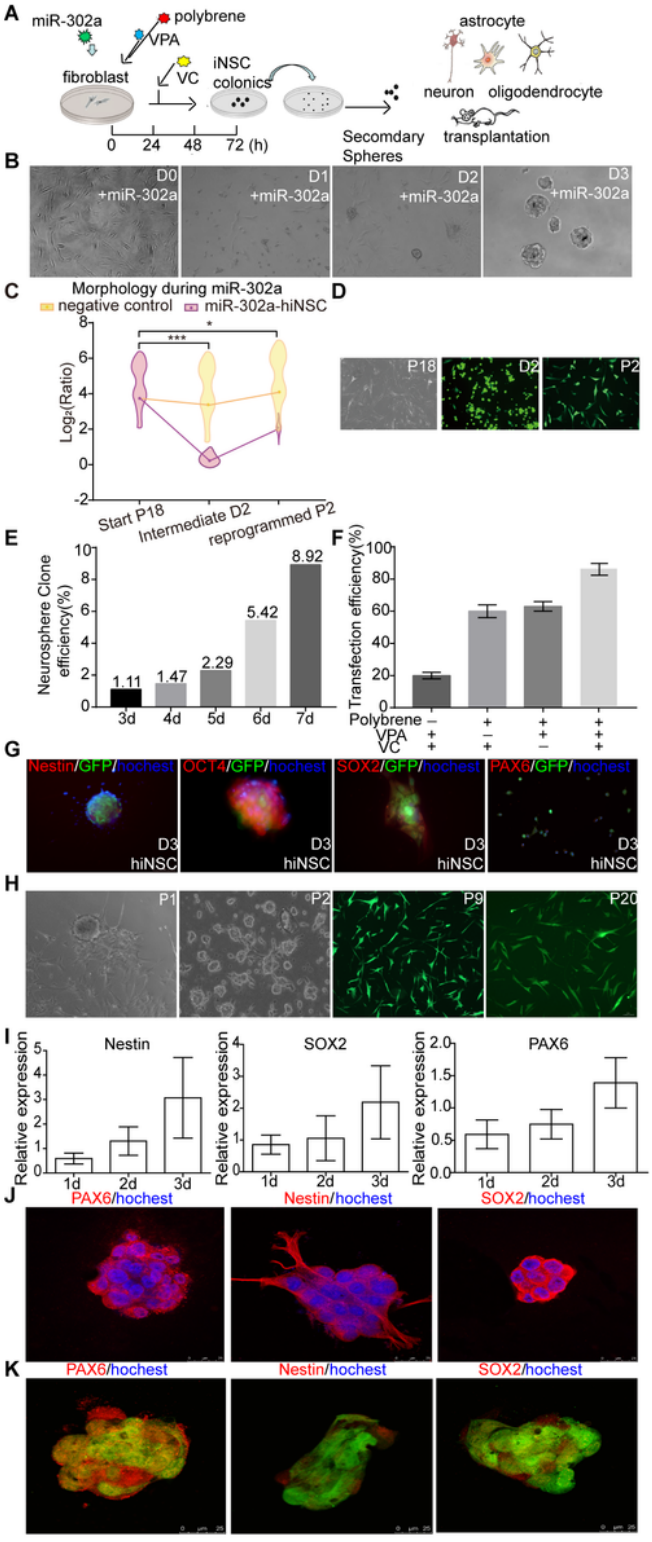

Figure 1

Generation and characterization of iNSCs from human postnatal foreskin-derived fibroblasts (HPFFs). A Schematic representation of the reprogramming process with single microRNAs miR-302a to generate neurospheres from human fibroblasts. **B** Phase-contrast images of HPFFs after overnight treatment with miR-302a virus vector in fibroblast medium. Has-miR-302a-infected cells spontaneously formed neurosphere-like colonies on gelatin-coated glass coverslip from 1-3 days after transfection. **C** The

circularity ratio of cells before, during, and after miR-302a reprogramming. The circularity ratio was calculated by dividing the maximum length by the vertical width. Fibroblasts became significantly rounder during MPTR. Data points represent the mean and are connected by lines. Significance was calculated using Tukey's test. *p < 0.05, ***p < 0.001. **D** Representative cells before, during, and after successful reprogramming are shown. GFP is shown in green. Scale bar, 100 um. **E** The colony formation efficiency of neurospheres generated by hiNSCs from human fibroblasts at 3, 4, 5, 6, and 7 days after miR-302a transfection. **F** Effect of the three small molecules used to increase transfection efficiency for reprogramming with has-miR-302a. Data are presented as mean ± SD (n=3). **G** Expression of Nestin, OCT4, SOX2, and PAX6 in hiNSCs neurospheres at day 3 after miR-302a transfection. **H** Neurospheres derived from miR-302a reprogrammed human fibroblasts can be expanded from P1 to P20 passages with adherent and suspension culture alternately. **I** RT-qPCR reveals that hiNSCs expressed typical NSC markers Nestin, SOX2, and PAX6 on day 3. **J** The control HPFFs infected with Ptf1a lentiviruses derived neurospheres were PAX6, Nestin, and SOX2 positive expression in Immunostaining. **K** Neurospheres induced from HPFFs by miR-302a were immunoreactive for PAX6, Nestin, and SOX2.

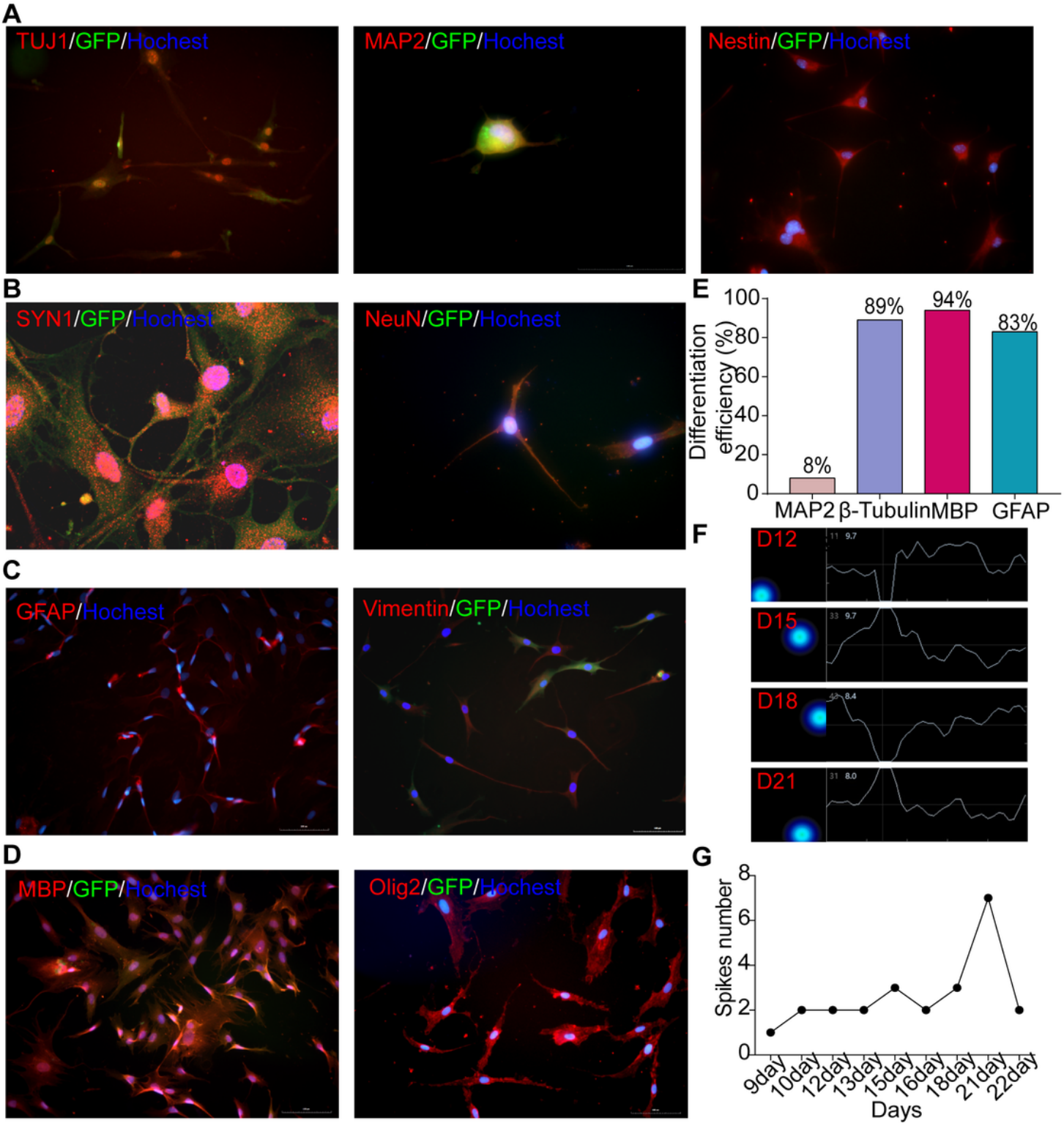

Figure 2

Multipotency of iNSCs in vitro. A hiNSCs could be differentiated into TUJ1+, MAP2+ and Nestin+ neurons by day 8 in culture after growth factor withdrawal. **B** hiNSCs were able to differentiate into SYN1+ and NeuN+ neurons. **C** hiNSCs differentiate into subtypes of astrocytes, including GFAP+ and Vimentin+ positive cells. **D** hiNSCs can robustly generate MBP+ and Olig2+ oligodendrocytes by day 22 in vitro. Scale bars represent 100 μM in A-D. **E** Quantification of MAP2, β-Tubulin, MBP and GFAP positive cells

rate differentiated from hiNSCs. **F** Cumulative activity map and spiking amplitude changes of differentiated neurons derived from hiNSCs at D12, D15, D18 and D21 using the MEA detection. **G** Quantification of the number of spike-positive electrodes of differentiated neurons with spontaneous action potential derived from hiNSCs on MEA increased from D12 to D21, and dropped on D22.

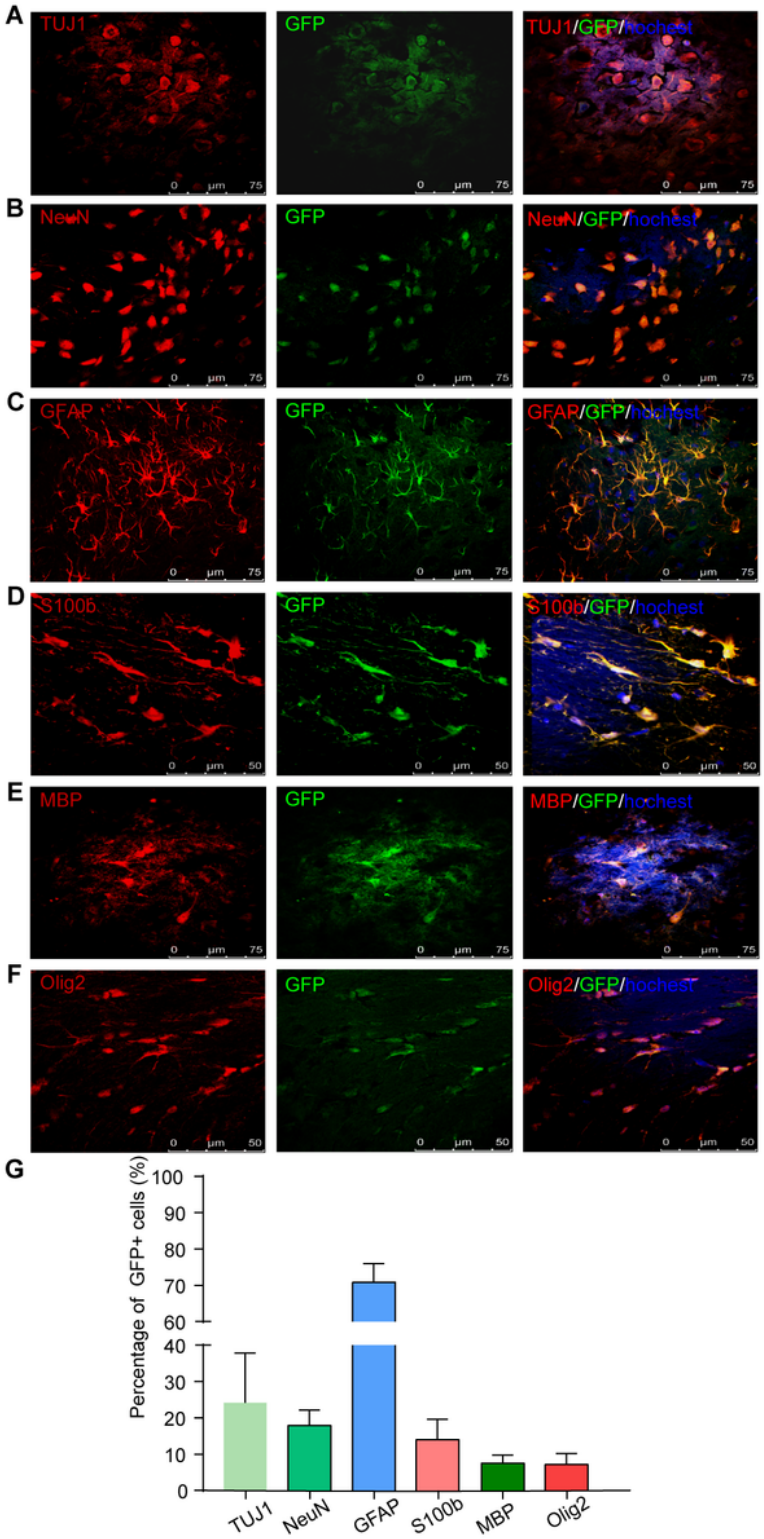

Figure 3

Mulitipotency of miR-302a-reprogrammed iNSCs in vivo. The miR-302a-reprogrammed iNSCs were injected into the striatum of 2-month-old nude mice (n=8). 3 weeks post-transplantation, GFP+ iNSCs migrated and integrated into the mice brain. **A-B**Immunostains reveal that hiNSCs can differentiate into TUJ1+ and NeuN+ neurons. **C-D** GFP+ iNSC can differentiate into GFAP+ and S100b+ astrocytes. **E** and**F** Injected GFP+ cells co-expressing the oligodendrocytes cell marker MBP and Olig2. **G** Quantification of labeled cells in the sections showed that GFP+ cells differentiated into TUJ1+, NeuN+, GFAP+, S100b+, MBP+, and Olig2+ cells. Scale bars represent 75 μM in **A**, **B**, **C**, and **E**, and 50 μM in **D** and **F**.

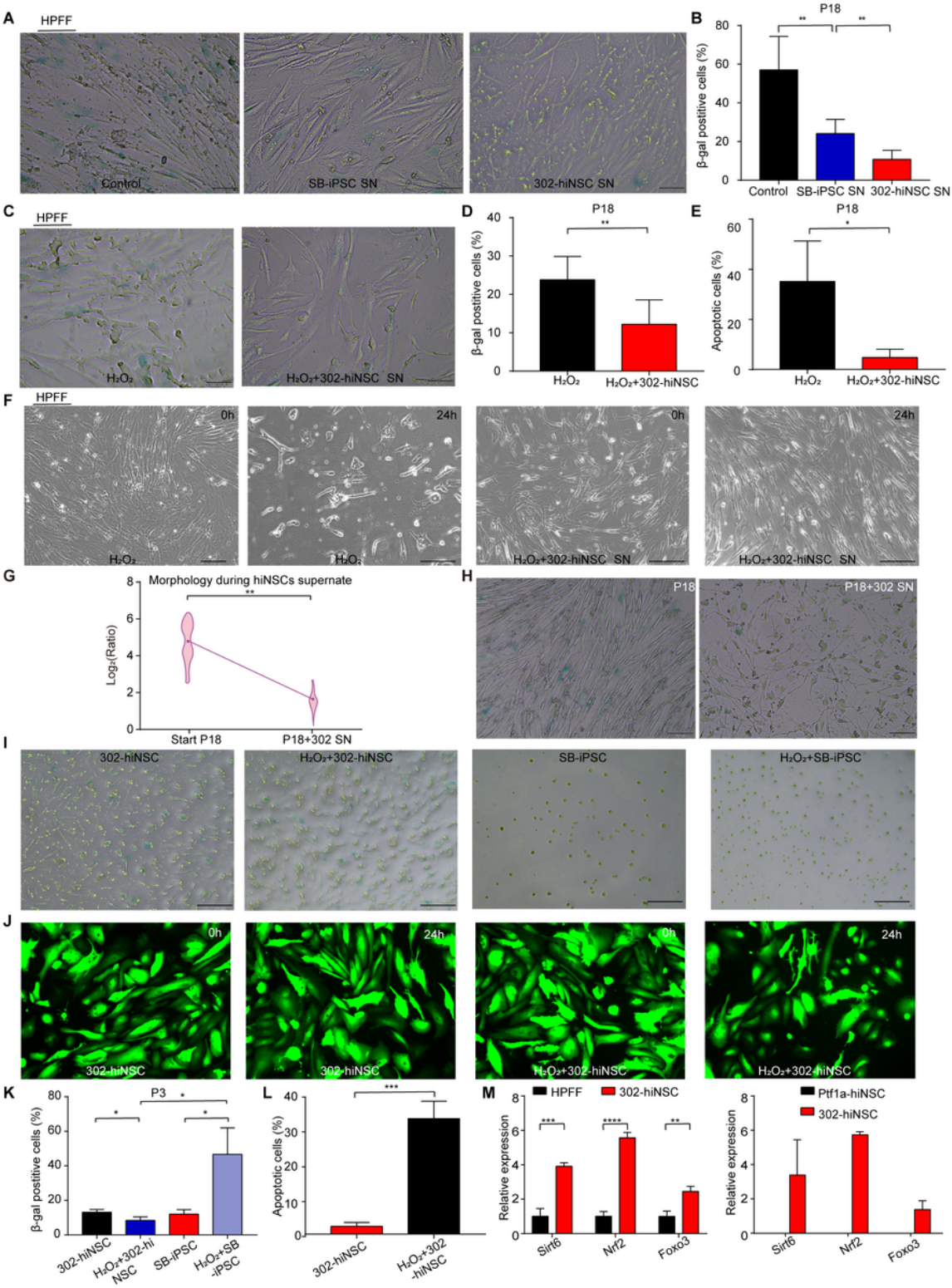

Figure 4

Anti-aging and antioxidant effects of culture supernatant from miR-302a-hiNSCs on senescent skin fibroblasts and NSCs. A β-gal staining analysis of HPFF, HPFF+SB-iPSC-iNSC SN and HPFF+miR-302a-hiNSC SN +H_2O_2 (P18). Scale bar, 100uM. **B** Quantitative analysis of β-gal staining of HPFF, HPFF+SB-iPSC-iNSC SN and HPFF+miR-302a-hiNSC SN+H_2O_2 (P18). Data are expressed as mean ± standard deviation. n=6, **p < 0.01, ***p < 0.001 (t-test). **C** β-gal staining analysis of HPFF+H_2O_2 and HPFF+miR-302a-hiNSC SN +H_2O_2 (P18). Scale bar, 100uM. **D** Quantitative analysis of β-gal staining of HPFF+H_2O_2 and HPFF+miR-302a-hiNSC SN+H_2O_2 (P18). Data are expressed as mean ± standard deviation. n=6, **p < 0.01 (t-test). **E** Quantitative analysis of apoptosis in HPFF treated with 300 mM H_2O_2 and HPFF cultured with miR-302a-hiNSC SN for 24 h. Data are expressed as mean ± standard deviation. n=6, *p < 0.05 (t-test). **F** Cell survival status under 24 h microscopy of HPFF treated with 300 mM H_2O_2 and HPFF cultured with miR-302a-hiNSC SN (P18). Specifically, HPFF cultured with miR-302a-hiNSC SN were resistant to H_2O_2-induced apoptosis. Scale bar, 200 uM. **G** Fibroblasts treated with miR-302a-hiNSC conditioned media. Fibroblasts became smaller after treatment with conditioned media. Data points represent the mean and are connected by lines. Significance was calculated using Tukey's test. **p < 0.01. **H** Representative cells before and after treatment with conditioned media are shown. Senescent cells are shown in green after staining with β-galactosidase. Scale bar, 100 um. **I** Analysis of β-gal staining of miR-302a-hiNSC, SB-iPSC-iNSC, miR-302a-hiNSC +H_2O_2 and SB-iPSC-iNSC +H_2O_2 with 300 mM H_2O_2 for 24h (P3), scale bar, 200uM. **J** MiR-302a-hiNSC were treated with 300 mM H_2O_2, and the amount of GFP-positive cells was observed after 24 h. Scale bar, 100 uM. **K** Quantitative analysis of miR-302a-hiNSC, SB-iPSC-iNSC, miR-302a-hiNSC +H_2O_2, and SB-iPSC-iNSC + H_2O_2. Data are expressed as mean ± standard deviation. n=6, *p < 0.05. **L** Amount of GFP - positive cells after treatment of miR-302a-hiNSC with 300 mM H_2O_2 for 24 h. Data are expressed as mean ± standard deviation. n=3, ***p < 0.001 (t-test). **M** qRT-PCR analysis of the expression of three longevity factors Nrf2, Sirt6 and Foxo3 in HPFF, Ptf1a-hiNSC and miR-302a-hiNSC. y-axis indicates the relative mRNA expression of the three longevity factors. n=3, **p < 0.01, ***p < 0.001, ****p < 0.0001 (t-test).

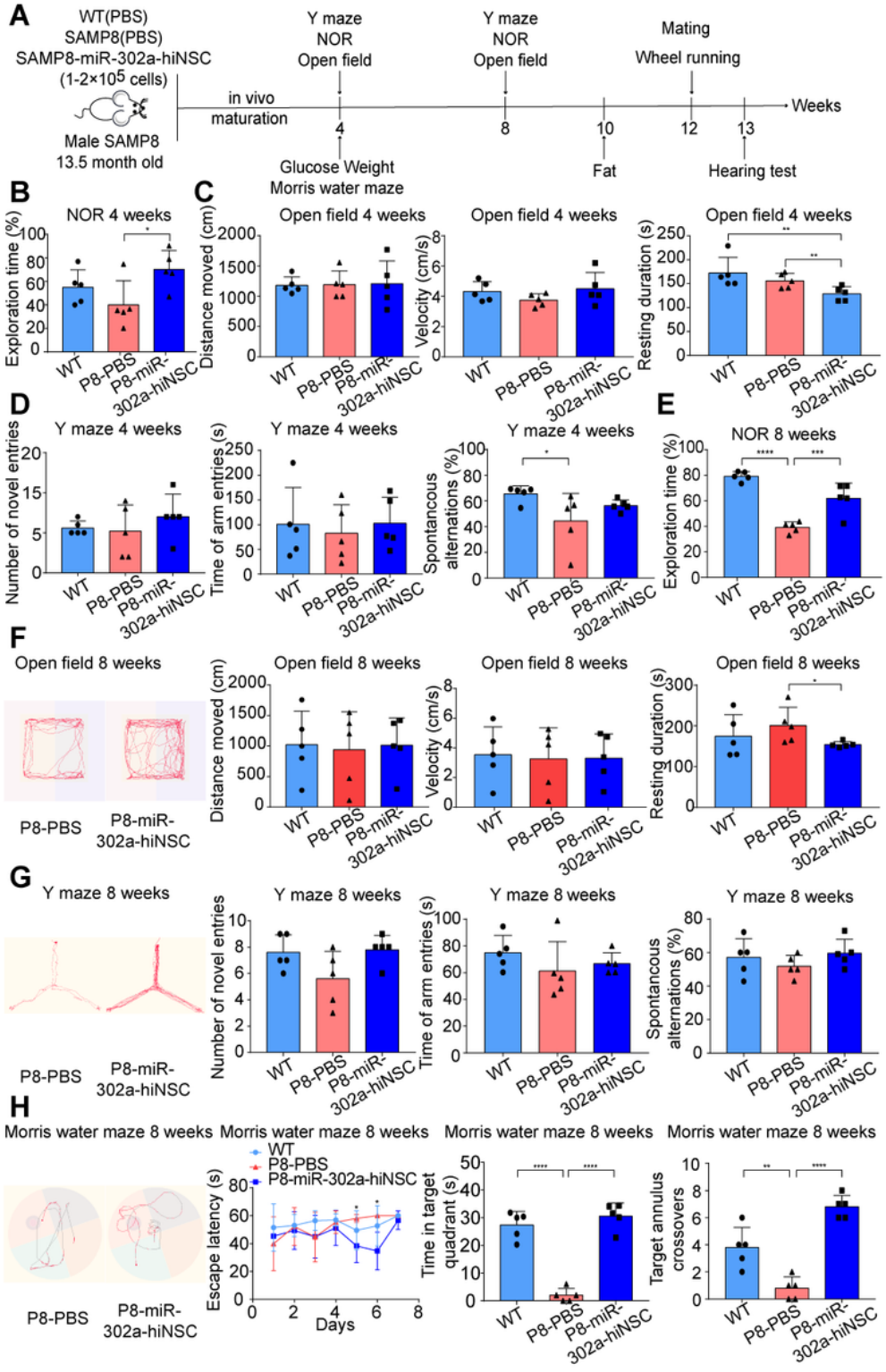

Figure 5

MiR-302a-iNSCs Improve Spatial Learning Ability and Memory in aged SAMP8 Mice. A Timeline for assessing the behavior of SAMP8 mice after transplantation of miR-302a-hiNSCs. **B** New object recognition at 4 w. New object recognition test recorded as a percentage of time spent exploring new objects in the three groups. *p < 0.05. **C** Open-field experiment at 4 w. Results of the three-group mine field test in WT, SAMP8 and miR-302a-hiNSCs transplanted mice. *p < 0.05, **p < 0.01. **D** Y-maze at 4w. There

was no improvement in the number, time and correct spontaneous alternating response (SAP) to explore the new dissimilar arm in the Y-maze. **E** New object recognition at 8w. The new object recognition test recorded the percentage of time spent exploring new objects for the three groups. **p < 0.01, ****p < 0.0001. **F**Open field experiment at 8w. Typical illustrative example of walking paths of SAMP8 and miR-302a-hiNSCs transplanted mice in the open field experiment in the mine field test. Results of three groups of WT, SAMP8 and miR-302a-hiNSCs transplanted mice in the mine field test. *p < 0.05. **G** Y-maze at 8w. Typical illustrative example of the walking pathway in SAMP8 and miR-302a-hiNSCs transplanted mice in the Y-maze test. number of times, time and correct spontaneous alternation response (SAP) to explore the new heterotopic arm did not improve in the Y-maze. **H** Morris water maze at 8w. Typical escape modalities in the Morris water maze test in SAMP8 and miR-302a-hiNSCs transplanted mice on day 7 hidden platform test. Learning curves for the Morris water maze acquisition test were obtained over a period of 6 days. 7d escape latency, time spent in the target quadrant and preference for target platform location were recorded for the Morris water maze experiment. *p < 0.05, ****p < 0.0001.

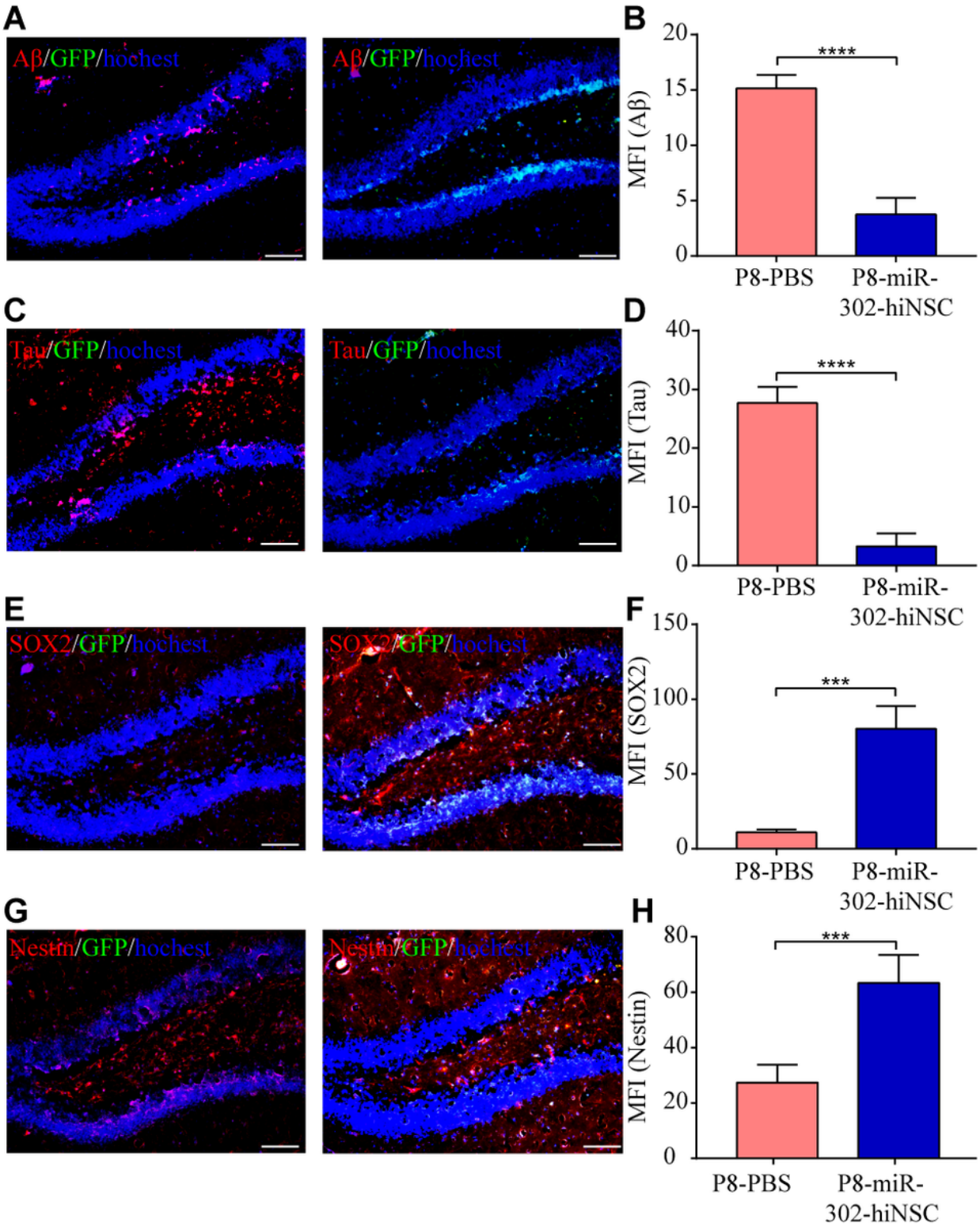

Figure 6

MiR-302a-hiNSCs regulate the expression of AD-related essential proteins in the SAMP8 mouse brain, restore endogenous neurons, and survive in the mouse brain for a long time. A Immunofluorescence of Aβ in the hippocampus of SAMP8 mice. Scale bar, 100 μm. **B** Mean fluorescence intensity of Aβ in the hippocampus of SAMP8 mice. ***p < 0.001. **C**Immunofluorescence of Tau in the hippocampus of SAMP8 mice. Scale bar, 100 μm. **D** Mean fluorescence intensity of Tau in the hippocampus of SAMP8 mice.

E Immunofluorescence of SOX2 in the hippocampus of SAMP8 mice. Scale bar, 100 μm. **F** Mean fluorescence intensity of SOX2 in the hippocampus of SAMP8 mice. **G** Immunofluorescence of Nestin in the hippocampus of SAMP8 mice. Scale bar, 100 μm. **H** Mean fluorescence intensity of Nestin in the hippocampus of SAMP8 mice. Data are presented as mean ± s.d. (n = 5).

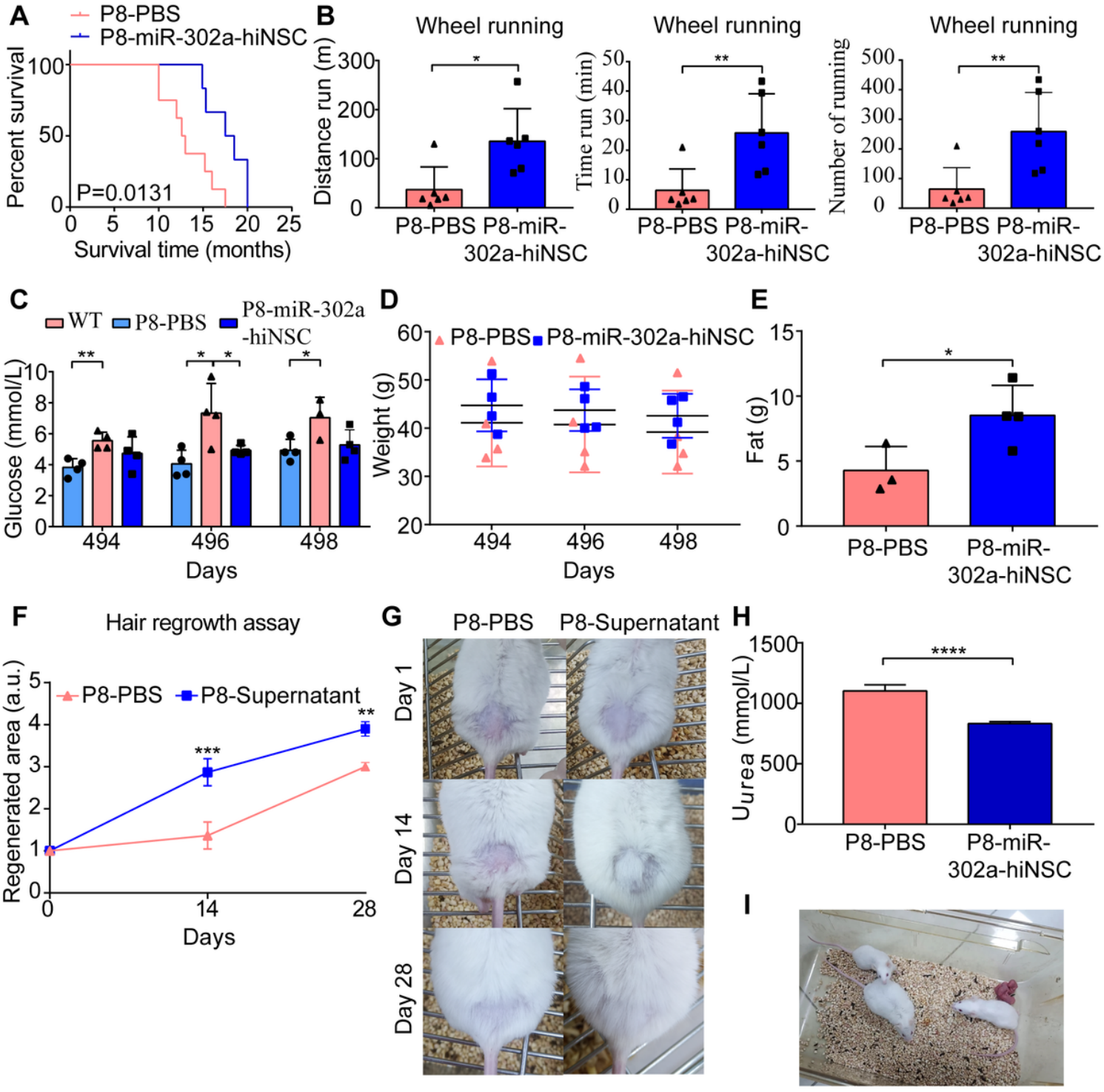

Figure 7

MiR-302a-hiNSCs improve fat, weight, blood sugar, hair and fertility in aged SAMP8 Mice. A Kaplan-Meier survival curves of SAMP8 mice and SAMP8+miR-302a-hiNSC mice. **B**Wheel running experiment in 16.5-month-old mice. Distance, time, and number of running wheel runs. **C** Blood glucose levels in WT, SAMP8 and SAMP8+miR-302a-hiNSC mice fasted for 12h. **D** Quantification of body weight in SAMP8 and SAMP8+miR-302a-hiNSC mice. **E**Plot of fat content in SAMP8 and SAMP8+miR-302a-hiNSC mice. **F** Quantification of hair regeneration capacity of mouse dorsal skin. a.u., arbitrary units. **G** Typical images of hair regeneration in male SAMP8 mice before and after 28 days of treatment with supernatant of PBS/miR-302a-hiNSC. **H** Quantification of urinary urea changes in SAMP8 and SAMP8+miR-302a-hiNSC mice. **I** miR-302a-hiNSC improves fertility in SAMP8 mice. 16.5-month-old SAMP8+ miR-302a-hiNSC mice are fertile after mating with BALB/c mice.

Supplementary Files

This is a list of supplementary files associated with this preprint. Click to download.

- SupplementaryFigures.docx
- SupportionInformation.docx